МІНІСТЕРСТВО ОСВІТИ ТА НАУКИ УКРАЇНИ

НАЦІОНАЛЬНИЙ АВІАЦІЙНИЙ УНІВЕРСИТЕТ

Кафедра конструкції літальних апаратів

ДОПУСТИТИ ДО ЗАХИСТУ
Завідувач кафедри
д-р техн. наук, проф.
_____ С. Р. Ігнатович
«_____» _____ 2021 р.

ДИПЛОМНА РОБОТА

(ПОЯСНЮВАЛЬНА ЗАПИСКА)
ЗДОБУВАЧА ОСВІТНЬОГО СТУПЕНЯ
"БАКАЛАВР"

Тема:«Аванпроект дальньомагістрального пассажирського літака пасаж ромісткістю 500людини»

Виконав: _____ Лю Кай

Керівник: к.т.н., доцент _____ С.С. Юцкевич

Нормоконтролер: к.т.н., доцент _____ С.В. Хижняк

Київ 2021

MINISRY OF EDUCATION AND SCIENCE OF UKRAINE
NATIONAL AVIATION UNIVERSITY
Department of Aircraft Design

APPROVED
Head of Department
Professor, Dr. of Sc.
_____S.R. Ignatovych
«___» _____ 2021

DIPLOMA WORK

(EXPLANATORY NOTE)
OF EDUCATIONAL DEGREE

«BACHELOR»

Theme: «Preliminary design of long range aircraft with a passenger capacity of 500 people»

Performed by: **_____ Liu Kai**

Supervisor: PhD, associate professor **_____ S.S. Yutskevych**

Standard controller: PhD, associate professor **_____ S.V. Khyzhnyak**

Kyiv 2021

NATIONAL AVIATION UNIVERSITY

Aerospace Faculty

Department of Aircraft Design

Educational degree «Bachelor»

Major 134 "Aviation and space rocket technology"

APPROVED
Head of Department
Professor, Dr. of Sc.
_____S.R. Ignatovych
«___» _____ 2021

TASK
for bachelor diploma work
LIU KAI

1. Theme: «**Preliminary design of long range aircraft with a passenger capacity of 500 people**»

Confirmed by Rector's order from 21.05.2021 year № 815/ст.

2. Period of work execution ____24.05.2021____ to ____16.06.2021____

3. Initial data:

- Prototype aircraft: Boeing 777-200ER, Boeing 787-10, Airbus A340-600;
- Maximum payload – 52.25 tons;
- Flight range with maximum payload – 8000 km;
- Cruise speed – 850 km/hour at operating altitude of 11 km;
- Landing speed – 232.3 km/hour.

4. Contents of explanatory note :

- Analysis of the specifications and characteristics of the prototype aircraft;
- Determination of the parameters of the designed aircraft;
- Mass calculation of the prototype aircraft and each component and instrument;
- Center of gravity calculation;
- Determination of aircraft layout;
- Choice and substantiations of the airplane scheme;

- Determination of basic flight performance;
- Description of the aircraft design;
- Engine selection;
- Special part;

5. List of the graphical materials:
   - general view of the aircraft (A1×1);
   - layout of the aircraft (A1×1);
   - assembly drawing of the floor panel (A1×1).

6. Calendar Plan

№ п/п	Task	Execution period	Signature
1	Task receiving, processing of statistical data	15.05.21	
2	Aircraft take-off mass determination	19.05.21	
3	Aircraft layout	19.05.21	
4	Aircraft centering determination	25.05.21	
5	Special part performing	06.06.21	
6	Graphical design of the parts	06.06.21	
7	Preliminary defense	09.06.21	
8	Completion of the explanation note		

7. Task date: «___» _____ 2021

Supervisor of diploma work _____ S.S. Yutskevych

Task for execution is given for _____ Liu Kai

ABSTRACT

Explanatory note to the diploma work «Preliminary design of long range aircraft with a passenger capacity of 500 people» contains:

72 sheets, 12 figures, 12 tables, 25 references and 3 drawings

Object of the design is development of a long range aircraft with a passenger capacity of 500 people.

Aim of the diploma work is the preliminary design of the aircraft and its design characteristic estimation.

The methods of design are analysis of the prototype aircraft and selections of the most advanced technical decisions with calculation the geometry for main parts of the aircraft: the wing geometry calculation, fuselage layout and landing gear design and the analysis of center of gravity position

The diploma work contains drawings of the long range aircraft with a passenger capacity of 500 people, calculations and drawings of the aircraft layout, analysis and design of aircraft floor panel.

PASSENGER AIRCRAFT, PRELIMININARY DESIGN, CABIN LAYOUT, CENTER OF GRAVITY DETERMINATION, FLOOR PANEL.

Format	№	Designation	Name	Quantity	Notes
			General documents		
A4	1	NAU 21 20L TT	Task of work	1	
	2		Long range passenger aircraft	2	
A1		NAU 21 20L 00 00 00 50 GV	General view		
A1		NAU 21 20L 00 00 00 50 FL	Fuselage layout		
A4	3	NAU 21 20L 00 00 00 50 EN	Long range passenger aircraft	72	
			Explanatory note		
A1	4	NAU 21 20L 53 00 00 50 AD	Documentation for assembly units	1	
			Floor panel		

Ch.	Sheet	Doc.№	Sign.	Date
Performed by		Liu Kai		
Supervisor		Yutskevych S.S.		
Adviser				
Stand. contr.		Khyzhnyak S.		
Head. of dep.		Ignatovych S.		

NAU 21 20L 00 00 00 50 EN

List of diploma work

List	Sheet	Sheets

AF 402 134

CONTENT

ABBREVAITIONS LIST

GDP	Gross Domestic Product
USD	United States Dollar
CAGR	Compound Annul Growth Rate
FAR-25	Federal Aviation Regulations: Part 25
CS-25	Certification Specification-25
CFRP	Carbon fiber reinforced polymer
MAC	Mean aerodynamic cord
NLG	Nose landing gear
MLG	Main landing gear
C.G.	Center of gravity
ASTM	American Society for Testing and Materials

INTRODUCTION

Air transportation accounts for a relatively small share of GDP (Gross Domestic Product), but is closely linked to other areas, particularly airports and aircraft manufacturing - collectively refferred to here as the “aviation industry”. Aviation industry is a key driver of many other economic activities. the Survey shows that the commercial aircraft market is valued at USD 85.3 billion in 2020 and is expected to reach USD 194.5 billion by 2026, growing at a CAGR (Compound annual growth rate) of 9.91% [1].

A wide-body aircraft is an aircraft with a fuselage wide enough to hold two aisles in the cabin. The advent of the twin-aisle jet has revolutionized air passenger transportation. Compared with ordinary narrow-body passenger aircraft, wide-body passenger aircraft in the aircraft size (wingspan, length, height, etc.) not much increase in the premise of the wing area and fuselage diameter has increased significantly, and thus the passenger (cargo) capacity, fuel capacity and range have been significantly improved. In addition, the cabin of a wide-body passenger aircraft is spacious and less oppressive, so it is more comfortable to ride, plus its cabin settings: there are two aisles, passengers in and out of the seat, walking around is also more convenient. In addition, wide-body airliners are usually heavier and less affected by airflow, so the flight is smooth, which also helps to improve the comfort of the ride. For these reasons, since its introduction in the early 1970s, wide-body airliners have been favored by airlines and passengers around the world, and have gradually become the mainstay of air passenger transportation worldwide. In today's world air passenger market, wide-body airliners are not only dominant on long-haul and intercontinental routes, but also widely used on short- and medium-haul routes [2].

Therefore, aircraft manufacturers need to continuously improve their wide-

body airliners to meet the ever-changing market requirements.

The objectives of the work are the preliminary design of a long-range aircraft with a capacity of 500 passengers and the analysis and optimization of the aircraft equipment.

The aircraft design process is based on the requirements of international airworthiness rules (FAR-25, CS-25) and current trends in the air transportation industry.

The special part of the work is about the analysis of the floor panel. The key idea of this design is to introduction of calculation methods to calculate the mechanical properties of aircraft floors when subjected to different kinds of loads, to facilitate the selection of the right flooring to suit the safety and comfort requirements.

PART 1

PRELIMINARY DESIGN OF THE AIRCRAFT

1.1. Analysis of the prototype aircraft

During the preliminary design phase, a more rigorous technical analysis of the preferred configuration from the conceptual design is performed. The goal of this phase is to find the optimal geometry for the aircraft based on commercial prospects and comparisons with competing aircraft. In this analysis process, all major aircraft parameters are considered variable. Moreover, parameters are critical in this phase and will directly affect the entire detailed design phase. It is common practice to establish a "baseline" configuration and perform a series of parametric studies around this layout.

While considering parametric studies, the design team will analyze competing aircraft, perform trade-off studies in detailed technical areas, our design process is no exception. Two manufacturers, European Airbus and U.S. aviation giant Boeing, divide the majority of the civil aviation market share. Their success is due to the fact that they have produced popular aircraft models with excellent performance. Therefore, the most efficient and secure approach to our design process is to draw on the key characteristics of these aircraft models that are appropriate to the needs of the aircraft being designed.

For the preliminary design, presented below, the prototype aircraft Boeing 777-200ER, Boeing 787-10 and Airbus A340-600 have been selected. The main parameters of the prototype aircraft are shown in Table 1.1 [3].

Table 1.1 – Statistic data of prototype aircraft

Parameter	Prototype aircraft		
	Boeing 777-200ER	Boeing 787-10	Airbus A340-600
The purpose of airplane	Passenger	Passenger	Passenger
Maximum take-off weight, m_{tow}, kg	297550	254011	380000
Maximum passenger capacity	440	440	440
Cruise altitude, km	11.6	11	11.1
Maximum payload, kg	56925	57277	66000
Flight Range, km	11000	12000	14450
Take off distance, m	3570	2800	3400
Landing distance, m	1615	1520	2063
Landing speed, km / h	251	260	240
Cruising speed, km/h	905	903	881
Number and type of engines	2×PW4090/RR 895/GE90-94B	2×GEnx-1B/RR Trent 1000	4×RR Trent 500
Pressure ratio	38	58.1	35
The form of the cross-section fuselage	Circular	Circular	Circular
Length of aircraft, m	62.78	63	75.3
Height of aircraft, m	18.5	17	17.3
Diameter of fuselage, m	6.2	5.77	5.64
Wingspan, m	60.9	60	63.45
Aspect ratio	8.67	10	9.3
Taper ratio	0.149	0.18	0.22
Sweepback on 1/4 chord, °	31.6°	32.2°	31.1°

The scheme of the aircraft includes the number, shape and relative position of its main structural elements - wings, empennage, fuselage, landing gears, as well as the the engines and their air intakes. The scheme of aircraft has an impact on the performance and characteristics of the aircraft and, finally, it determines the overall efficiency of the aircraft. The scheme of each aircraft can be described by its type, operating conditions and the primary requirements of the aircraft design. The key issues to be addressed when selecting the aircraft scheme are to meet the performance requirements in the best way possible, which is to get a scheme of minimum amount of airframe and takeoff weight under the premise of safety and reliability, maximum lift-to-drag ratio and maximum aerodynamic efficiency.

Aerodynamic performance depends mainly on the layout of the main components of the aircraft. Therefore, the placement of payload, fuel power plants and miscellaneous equipment should be considered when developing the aircraft scheme solution.

By analyzing the statistics of the latest generation airplanes presented in the table above, cutting-edge information obtained will show the tendency of aircraft design and thus meet the aerodynamic and economic requirements in a most efficient way.

Decisions made during the formation of the shape of the aircraft are important because mistakes made at this stage are very difficult to correct. Therefore, the choice of aircraft scheme and its parameters should be considered thoroughly and reasonably; especially those important parameters that have the greatest impact on the aerodynamic performance of the aircraft.

1.2. Brief description of the designed aircraft

An airplane is made up of several main parts. It mainly consists of wing, fuselage, tail unit, engines, landing gears and control surfaces. In order to make the most optimal decisions about the configuration of various parts of an aircraft, the

designer must fully understand the functions of each part. Each aircraft part is interrelated to and interacts with the functions of other parts.

Similar to the structure of the prototype aircraft Boeing 777-200ER, designed aircraft is a wide-body low-wing aircraft with swept-back trapezoid wings and conventional type of tail unit. The four engines are mounted under the wings, and the two main landing gears are also located under the wings when extended.

1.2.1. Wing

The main function of the wing is obviously to make the aircraft fly by generating lift. The wing also produces two other unwanted aerodynamic products: an aerodynamic drag and an aerodynamic pitch moment. In addition, the wing is an important component in providing the lateral stability of the aircraft, which is critical to flight safety. The ailerons of conventional aircraft are mounted on the outboard part of the trailing edge of the wing, and the force arm relative to the longitudinal axis is very large when the force is applied. Therefore, the wing has a great influence in providing lateral control of the aircraft.

The wings are made of aluminum alloy, which can reduce the structural weight of the aircraft, as well as improve the performance of the aircraft from the aspect of durability and reliability. The wing of the designed aircraft is composed of many materials: a7000 series aluminum alloy for the upper wing and a2000 series aluminum alloy for the lower wing.

The aircraft is designed with a two-spar structure and is made of composite materials similar to that of Boeing 777X, which allows for a good balance between structural strength and structural weight. In an aircraft wing, the wing spar is one of the most important force-bearing elements, generally consisting of caps and web. The main function is to bear the bending moment and shear force, the upper and lower edge strips of the beam bear the axial force caused by the bending moment, while the shear force is mainly borne by the web. The airplane is designed with a web type wing beam, the root of which is fastened to the fuselage and is the main

longitudinal bearing member of the wing, bearing most of the bending moment of the wing. The web wing beam is simple in construction, has good force characteristic , and can also be used as a bulkhead for the overall fuel tank.

Most turbofan-powered civil transport aircraft have low wings, the designed aircraft is no exception. The advantages of low wing configuration are:

1) Structurally simple, the main structure of the wing can pass under the passenger cabin floor, thus making the wing-fuselage connection relatively easy.

2) Landing gear can be short and simple. Bigger wheel track improves taxiing stability (especially in high winds) and is less vulnerable to structural failure. Engines mounted under the wing and flaps are easier for maintenance personnel to repair on the ground.

3) The wing is one of the strongest components of the aircraft, protecting the fuselage in the event that the aircraft hits the ground or water. In the case of a forced landing at sea, the wing can also float on the surface of the water so that the fuselage does not sink like underwater, thus buying time for emergency evacuation.

4) The take-off distance can be reduced thanks to a more pronounced ground effect.

Many of these features make low-wing configuration the perfect solution for the designed aircraft.

When the aircraft is in transonic flight, the aircraft will encounter great wave drag. At this point, the aircraft will either have difficulty in increasing speed, or will not be able to withstand the huge impact and break into pieces. In order to overcome and reduce the wave drag, people changed the straight wing shape and came up with the swept-back wing design. Because the cruise speed of the designed aircraft is in the transonic category, the swept-back wing design is used, as is the case with most civil airliners on the market. Of course, the swept-back wing design was chosen not only for the above reasons. The wings of the designed aircraft is being swept for the five design objectives below [4]:

1) Improved wing aerodynamic performance (lift, drag, pitching moment) at transonic, supersonic and hypersonic speeds through delayed compressibility effects.

2) Optimized center of gravity position of the designed aircraft.

3) Improved static lateral stability.

4) Enhanced longitudinal and directional stability.

5) Increased pilot view.

In addition, the designed aircraft is equipped with winglets. Since there is a considerable pressure difference between the lower and upper surfaces of the wing, wingtip vortices are generated at the wingtips. These wingtip vortices then curl up and around the local edges of the wing, thus reducing the lift at the wingtip region, which will manifest itself as a reduction in effective wingspan. To avoid this loss, winglet were created. Winglets are small, near-vertical lift surfaces mounted backward or downward relative to the wingtip.

1.2.2. Fuselage

Generally speaking, the fuselage is mainly used to accommodate the crew, passengers, baggage and cargo. Passengers are housed in the passenger cabin and cargo is housed in the cargo hold. Large pieces of luggage are also stored in the cargo hold, while smaller pieces of luggage are brought into the passenger cabin as carry-on luggage and stored in the stowage compartment above the seats. The cockpit and primary aircraft systems are also located in the fuselage.

The main type of fuselage structure is the semi-monocoque structure. This structure provides a better strength-to-weight ratio for the central part of the aircraft fuselage compared to monocoque structures. Aluminum makes up the largest portion of all the materials that make up the fuselage of the designed aircraft, such as the a7000 series aluminum alloys. The fuselage as a beam consists of longitudinal units (longerons and stringers), transverse units (frames and bulkheads) and the external skin.

The shape of the fuselage cross-section mainly depends on the structural requirements of the pressurization. The circular shell responds to internal pressure loads by means of circumferential stress. This makes the circular cross section efficient and therefore the lowest structural weight. Any non-circular shape imposes bending stresses in the shell structure. This will add considerable weight to the body structure. So the circular cross section strike a balance in all aspects for the designed aircraft.

1.2.3. Tail Unit

The empennage is a kind of device mounted on the very tail of an aircraft that enhances flight stability while providing directional control. Most empennage include horizontal stabilizers, vertical stabilizers, elevators and rudders. The primary criterion for tailplane design is to offer sufficient stability and controllability to the aircraft. It solves the problem of providing sufficient moment for the aircraft's center of gravity to counteract the moment generated by the lift on the wing, through the principle of leverage, thus keeping the aircraft stable.

The main function of the horizontal stabilizer is to trim the aircraft from the longitudinal direction by the aerodynamic force. In addition, it is an important component in providing longitudinal stability, a requirement critical to aircraft safety. In most aircraft, the elevator is a moving part of the horizontal stabilizer, so maneuverability and longitudinal control are achieved through the horizontal stabilizer.

Likewise, The main function of the horizontal stabilizer is to trim the aircraft directionally by the generated aerodynamic force. In addition, it is an important component in providing longitudinal stability, a requirement critical to aircraft safety. In most aircraft, the rudder is a moving part of the vertical stabilizer, so maneuverability and directional control are achieved through the vertical stabilizer. The vertical stabilizer of the designed aircraft uses horn balance to balance the hinge moment.

The 777 empennage consists of the horizontal and vertical stabilizers, and they have elevators and rudder installed on them respectively. Each stabilizer is configured as a two-cell box consisting of a main structural box and an auxiliary or forward torque box, leading edges, tip, and fixed trailing edges. The main torque boxes are made from CFRP composite material. The structure consists of solid-laminate front and rear spars, honeycomb sandwich ribs, and integrally stiffened laminate skin panels. A toughened matrix CFRP material is used for the main box panels and the main box spars. This material provides improved resistance to impact damage over previous materials. The auxiliary torque box and fixed trailing edges are made of glass or glass/carbon fiber reinforced plastic sandwich panels and aluminum ribs. The leading edge, tip, and auxiliary spar are aluminum construction [5]. Thus, the designed aircraft has a empennage of similar construction and material to the prototype aircraft Boeing 777.

1.2.4. Engines

The CF6-50 series engines are high-bypass ratio turbofan engines developed by General Electric after the 1970s to meet the requirements of further reducing fuel consumption and improving reliability of large wide-body airliners. The large fan diameter allows the engine to improve propulsion performance while further reducing fuel consumption rates. This engine is also equipped with a three-booster stage, so it has a new aerodynamic performance, which makes the amount of air flow increased. In addition, the engine's load-bearing frame and nacelle structure have been reinforced to accommodate the increased thrust.

The air flow circulation part adopts special type surface, three-dimensional flow and new blade design in rotor and static sub-blade, active clearance control technology is adopted in all high and low pressure turbines, and welding, no margin forging and casting blank, composite material, and new technology are widely adopted, which results in low fuel consumption rate, light weight, low number of parts, and easy maintenance. The use of full power digital electronic control system further reduces the fuel consumption rate.

1.2.5. Landing Gears

The aircraft landing gear bears the full weight of the aircraft during takeoff and landing as well as the impact load at the moment of takeoff and landing. They are usually mounted under the wings or under the fuselage.

Just like the mainstream large airliners on the market, the designed aircraft uses conventional tricycle-type landing gear. Tricycle landing gears for large aircraft offer the following advantages:

1) Provide more powerful brakes while ensuring that the aircraft does not flip over on the nose during braking, this making higher landing speeds possible.

2) Provide better visibility to the flight deck, especially during landing and maneuvers.

3) Prevents the aircraft from circling on the ground. Since the center of gravity of an aircraft is generally located in front of the main landing gear, the force acting on the center of gravity will tend to move the aircraft forward rather than spin around.

As the aircraft speed increases, parasitic drag increases. The mechanics of stowing and retracting the landing gear to avoid the impact of parasite drag on the performance of the aircraft. As the aircraft speed increases, the drag caused by the landing gear increases, and a method of retracting the landing gear to eliminate parasitic drag is needed for our designed aircraft despite the weight of the mechanics.

The designed aircraft uses six wheel main landing gear system. The six-wheel design makes the fuselage more stable. The dual-wheel nose landing gear is a gigantic component in order to effectively control two sets of 6-wheel main landing gear tires without the need for additional rear axle mounts. This structure not only efficiently distributes the weight of the aircraft on the runway and taxiing area, but also enables the aircraft to have no more than three landing gear struts, eliminating the need to add two landing gear under the mid-fuselage.

1.2.6. Control Surfaces

The main flight control surfaces of the designed aircraft include: ailerons, elevator and rudder. The ailerons are mounted on the outboard portion of the trailing edge of the wing and allows the aircraft to rotate around the longitudinal axis when deflected. The elevator is mounted on the trailing edge of the horizontal stabilizer. When it is deflected, it changes the pitch angle of the aircraft, that is, the attitude about the horizontal or lateral axis of the aircraft. The rudder is hinged on the trailing edge of the vertical tail, and the partial span tab is mounted below the rudder. It allows the aircraft to rotate around the vertical axis when deflected.

Other control surfaces include flaperon, trailing edge flaps, leading edge slats and double-slotted flaps mounted in the inboard position. The flaps can achieve the role of flaps and ailerons simultaneously, while the other devices act as high lift devices to increase the lift coefficient and improve the aircraft's critical angle of attack during deflection. Last but not least, the spoilers mounted on the wings are used for two main functions, to reduce lift while increasing drag and to rotate the aircraft around the longitudinal axis in conjunction with the flaps. When used as speed brakes or landing spoilers, they will deploy on both wings simultaneously.

The flight crew transmits control and maneuvering directive by electrical wires and amplify them by computer, sending them directly to the hydraulic actuators in the elevator, rudder, ailerons and other control surfaces. This three-axis "fly-by-wire" flight control system reduces weight, simplifies factory assembly, and requires less spare parts and maintenance in air service than traditional mechanical systems that rely on steel cables.

1.3. Substantiation of the new aircraft parameters

1.3.1. Wing geometry calculation

The first step in calculating the geometric characteristics of an aircraft wing is to first select the takeoff weight m_o and the specific wing load P_o, where the specific wing load can be obtained by analyzing similar prototype aircraft.

For the designed plane, the specific wing load P_o was chosen to be equal to $5808\ N/m^2$.

From this:

Full wing area with extensions is:

$$S_{wfull} = \frac{G_o}{P_o} = \frac{m_o \cdot g}{P_o} = \frac{322080 \cdot 9.8}{5808} = 543.45\ (m^2)$$

The relative wing extensions area of the designed aircraft is 0.1.

Wing area is:

$$S_w = 543.45 \cdot (1 - 0.1) = 489.11\ (m^2)$$

A fundamental parameter of the wing is the aspect ratio. Generally speaking, the larger the aspect ratio of the wing, the better the aerodynamic performance of the aircraft. As the aspect ratio increases, the maximum lift coefficient of the wing increases, resulting in a decrease in the induced drag of the wing, which is inversely proportional to the aspect ratio. But at the same time, the increased wing length makes the wing load larger, in order to ensure the integrity of the structure, and the need to apply more reinforcement structure, then the lightness of the aircraft can not be guaranteed

Examples of the aspect ratios of some passenger aircraft are presented in table 1.3.

Table 1.3 – Statistic data of prototype aircraft

№	**Aircraft type**	**Aspect ratio**
1	2	3
1	Boeing 777-200ER	8.67
2	Boeing 787-10	10
3	Airbus A340-600	9.3
4	Boeing 747-400	7.7

1	2	3
5	Boeing 737-800	9.44
6	Airbus A321	10
7	Airbus A330	10.06
8	Boeing 767-300ER	8

For designed plane the value of aspect ratio 7.39 is selected.

Wing span is:

$$l_w = \sqrt{S_w \cdot \lambda} = \sqrt{489.11 \cdot 7.39} = 60.12\ (m^2)$$

Where λ is the aspect ratio;

Root chord is:

$$b_o = \frac{2S_w \cdot \eta_w}{(1+\eta_w) \cdot l_w} = \frac{2 \cdot 489.11 \cdot 3.6}{(1+3.6) \cdot 60.12} = 12.73\ (m)$$

Where η_w is the taper ratio;

Tip chord is:

$$b_t = \frac{b_o}{\eta_w} = \frac{12.73}{3.6} = 3.54\ (m)$$

Maximum wing width is determined in the forehead i-section and by its span it is equal:

$$c_i = c_w \cdot b_t = 0.12 \cdot 3.537 = 0.43\ (m)$$

Board chord is:

$$b_{ob} = b_0 \cdot \left(1 - \frac{(\eta_w - 1) \cdot D_f}{\eta_w \cdot l_w}\right) = 12.73 \cdot \left(1 - \frac{(3.6-1) \cdot 7}{3.6 \cdot 60.12}\right) = 11.66\ (m)$$

Where D_f is the fuselage diameter.

Some other fundamental parameters of the wing are also determined in the following.

The taper ratio is the second of the three most important geometrical characteristics of a wing, and that of the designed aircraft has been selected to be 3.6 according to the following considerations [4]:

1) Wing taper changes the lift distribution of the wing. It is a useful approach to improve the lift distribution of the wing so it is considered an advantage of taper, since one of the goals of wing design is to generate lift so that the spread lift distribution is elliptical.

2) The wing taper reduces the bending moment at the wing root while reducing the weight of the wing, because the center of gravity of both wings will move towards the longitudinal axis of the aircraft with the wing taper.

3) The wing taper will bring more cost to the wing manufacturing due to its relatively complex internal structure.

4) The wing taper reduces the mass moment of inertia of the wing about the longitudinal axis of the aircraft, thus improving the lateral control of the aircraft.

5) The wing taper usually gives the wing a swept-back angle, which improves the lateral stability of the aircraft.

6) The wing taper gives the aircraft adequate space to accommodate the gigantic main landing gear of the designed aircraft.

As mentioned above, the taper ratio has a wide variety of effects on aircraft performance. The final determination of the wing taper ratio is made through detailed calculations and estimation of the aircraft's performance, stability, controllability, manufacturability and cost.

The thickness-to-chord ratio has been selected to be 0.12 because [4]:

1) The thickness-to-chord ratio affects the profile drag on the wing, the greater the thickness, the greater the drag, the greater the drag, and too much increase in thickness can offset the reduction in induced drag caused by high AR.

2) The thickness-to-chord ratio affects the lift coefficient of the wing, and for high subsonic passenger aircraft, the optimal lift coefficient is between 9% and 12%;

3) The greater the thickness the greater the stall angle of attack.

4) Under the premise of ensuring good stall characteristics, the value of the maximum relative thickness should be as small as possible, and the position of the maximum relative thickness should be close to the trailing edge to obtain good airfoil performance.

The sweepback angle on the quarter chord line is selected to be 30° . The formation of shock not only causes a dramatic increase in drag; it also changes the chordal pressure distribution of the airfoil, shifting the center of lift from about a quarter chord of the airfoil to the center chord. The result is called "Mach-tuck", which is a severe increase in pitching moment downward from the nose.

When deciding on the scheme of the wing, the number and position of the wing spars and the position of the wing.

Most wing structures have two wing spars, the leading wing spar and the trailing wing spar. The front wing spar is located near the leading edge and the trailing wing spar is about two-thirds of the way from the trailing edge. The two spars scheme is selected, which is presented in the figure below(Fig 1.1).

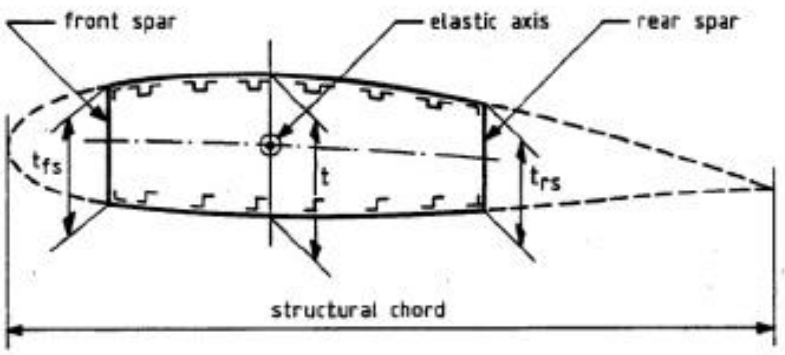

Fig. 1.1 Two spars wing design

The mean aerodynamic chord values are obtained by applying the geometric method as follows: $b_{MAC} = 8.98$ (m). And the final result are shown in Figure 1.2.

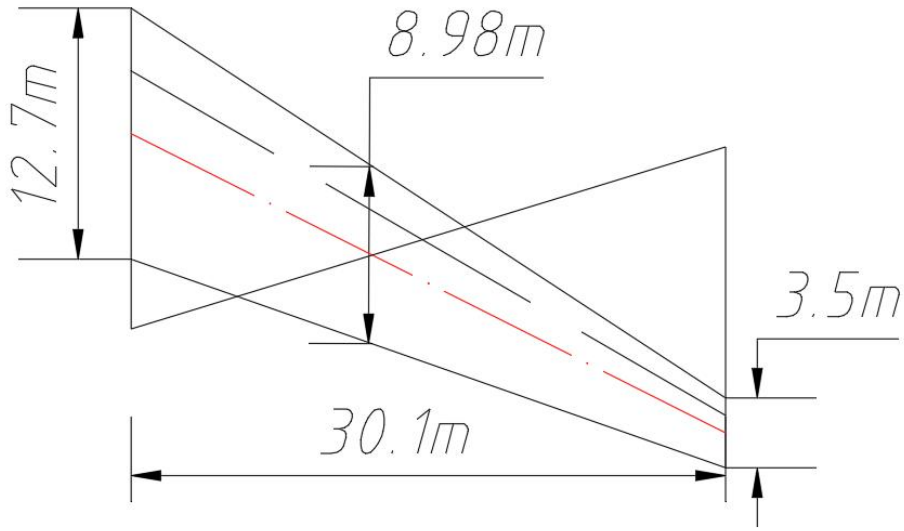

Fig 1.2 Geometrical method of wing mean aerodynamic chord determination

The next step is to determine the main parameters of the ailerons and high-lift devices.

Aileron geometry parameters are determined as follows:

Ailerons span:

$$l_{ail} = 0.3 \cdot \frac{l_w}{2} = 0.3 \cdot \frac{60.121}{2} = 9.02\ (m)$$

Ailerons chord:

$$b_{ail} = 0.25 \cdot b_i$$

Aileron area:

$$s_{ail} = 0.065 \cdot \frac{s_w}{2} = 0.065 \cdot \frac{489.11}{2} = 15.9\ (m^2)$$

The trend in modern aircraft design is to reduce the relative wingspan and aileron area. In this case, spoilers are also used to act as ailerons in order to provide lateral control of the aircraft.

Aerodynamic balance of the aileron:

Axial $S_{axinail}$:

$$S_{axinail} = 0.26 \cdot S_{ail} = 0.26 \cdot 15.9 = 4.13\ (m^2)$$

Inner axial compensation $S_{inaxinail}$:

$$S_{inaxinail} = 0.3 \cdot S_{ail} = 0.3 \cdot 15.9 = 4.77\ (m^2)$$

Area of ailerons trim tab for four engine airplane:

$$S_{tt} = 0.075 \cdot S_{ail} = 0.075 \cdot 15.9 = 1.19\ (m^2)$$

Range of aileron deflection

Upward $\delta_{ail}^{'} \leq 30°$;

Downward $\delta_{ail}^{''} \leq 10°$.

The purpose of determining the geometric parameters of the wing high-lift device is to provide the wing lift coefficient for takeoff and landing.

The high lift system with light weight and low complexity is required to enable the aircraft to achieve high lift.

1) Excellent climbing performance at takeoff, including high temperatures and high conditions, to meet the requirements of low drag.

2) Low approach speed to ensure safe approach, large wing area resulting in medium maximum lift (Cl_{max}) requirements.

3) Good control quality (landing attitude, pitch characteristics, roll ability, etc.).

4) Good tail-vortex characteristics.

Taking into account the design of the prototype aircraft and the current trend of high-lift devices, a hybrid design of single-slotted flaps and double-slotted flaps has been chosen.

$$b_{fl} = 0.29 \cdot b_t = 0.29 \cdot 3.54 = 1.03\ (m)$$

Before the next calculation, it is necessary to select among the available airfoils and thus determine the value of the lift coefficient $C_{y\,max\,bw}$ and determine the increment of this coefficient $C_{y\,max}$ for the high-lift devices calculated as follows:

$$\Delta C_{y\,max} = \left(\frac{C_{y\,max\,l}}{C_{y\,max\,bw}}\right)$$

where $C_{y\,max\,l}$ – the necessary lift coefficient of the wing when the aircraft is landing (determined when selecting aircraft parameters).

The relative chord ratio of typical wing high-lift devices are:

$b_f = 0.28..0.3$ – single-slotted and double-slotted flaps;

$b_s = 0.1..0.15$ – slats.

1.3.2. Fuselage Layout

The main parameters of the fuselage, which is an important component to accommodate the payload and provide a comfortable and safe environment, need to be determined.

For the designed aircraft, the length of the nose part must be:

$$l_{nfp} = 1.8 \cdot D_f = 1.8 \cdot 7 = 12.6\ (m)$$

Since the aircraft designed is pressurized, a round fuselage is best because it is the most efficient in carrying hoop stress.

Fuselage length is equal:

$$l_f = \lambda_f \cdot D_f = 10 \cdot 7 = 70\ (m)$$

Fuselage nose part aspect ratio is equal:

$$\lambda_{fnp} = \frac{l_{fnp}}{D_f} = \frac{12.6}{7} = 1.8$$

Sum of nose and rear parts must be equal 4.8.

Length of the rear part of the fuselage is equal:

$$\lambda_{frp} = 4.8 - \lambda_{fnp} = 3\ ;$$

Length of the fuselage rear part is equal:

$$l_{frp} = \lambda_{frp} \cdot D_f = 3 \cdot 7 = 21\ (m)\ ;$$

For passenger aircraft, the height of the cabin is one of the important parameters of the midsection of the fuselage.

For long range airplanes: the height as: $h_1 = 1.9\ m$; passage width $b_p = 0.55\ m$; height of the window $h_2 = 1\ m$; area for luggage $h_3 = 1.2\ m$.

Cabin height is equal:

$$H_{cabin} = 0.296 + 0.383 \cdot B_{cabin} = 0.296 + 0.383 \cdot 6.64 = 2.84\ (m)$$

As mentioned above a round body can efficiently cope with loop stresses and therefore has the lowest structural weight. Any non-circular shape will create bending stresses in the shell structure, which will add weight to the fuselage structure. However, a perfectly circular cross section may not be the best shape for enclosing the payload because it may provide too much unusable volume above or below the nacelle space. In some designs, this problem can be solved by using several horizontal or vertical circular sections to form a cross-sectional layout.

The spacing between the frames of the fuselage is 508mm according to the prototype aircraft Boeing 777-200ER [16].

The shape of the window is rectangular with the rounded corners with a diameter of 300...400mm.

In economy class, configuration of 3+(2+2)+3 in a row is chosen, and taking into account the width of the fuselage, the cabin width can be calculated as:

$$B_{cabin} = n_{3chblock} \cdot b_{3chblock} + n_{2chblock} \cdot b_{2chblock} + n_{aisle} \cdot b_{aisle} + 2\delta$$
$$= 2 \cdot 1560 + 2 \cdot 1060 + 2 \cdot 550 + 2 \cdot 150 = 6.64\ (m)$$

The length of passenger cabin is equal:

$$L_{cabin} = 3 \cdot L_1 + (n_{raws} - 1) \cdot L_{seatpitch} + 3 \cdot L_2$$
$$= 3 \cdot 1200 + (50 - 1) \cdot 810 + 3 \cdot 300 = 44.19\ (m)$$

1.3.3. Luggage compartment

Given the fact that the unit of load on floor $K = 977\ (kg/m^2)$

The area of cargo compartment is defined:

$$S_{cargo} = \frac{M_{bag}}{0.4K} + \frac{M_{cargo\&mail}}{0.6K} = \frac{20 \cdot 500}{0.4 \cdot 977} + \frac{15 \cdot 500}{0.6 \cdot 977} = 38.4\ (m^2)$$

Cargo compartment volume is equal:

$$V_{cargo} = \nu \cdot n_{pass} = 0.2 \cdot 500 = 100\ (m^3)$$

Luggage compartment design similar to the prototype.

1.3.4. Galleys and buffets

The aircraft's galley includes facilities to store and carry food and beverages, as well as equipment used by flight attendants in case of emergency. Due to the long flight duration of the designed aircraft, the galley must be able to supply passengers with at least two meals. Galley cabinets need to be placed in the kitchen space separated by separate doors. Food and drinks cannot be placed next to toilet facilities and wardrobe.

Volume of buffets(galleys) is equal:

$$V_{galley} = 0.1 \cdot 500 = 50\ (m^3)$$

Area of buffets(galleys) is equal:

$$S_{galley} = \frac{V_{galley}}{H_{cab}} = \frac{50}{2.839} = 17.6\ (m^2)$$

Number of meals per passenger breakfast, lunch and dinner – 0.8 kg; tea and water – 0.4 kg;

If food organized once it is given a set number 1 weighing 0.62 kg. Food passengers appears every 3.5 hour flight.

The design of the Galley is similar to the prototype aircraft.

1.3.5. Lavatories

The number of toilet facilities is determined by the duration of the flight and the passenger capacity: with $t > 4h$, one toilet for 40 passengers.

The number of lavatories can be estimated as follows:

$$n_{lav} = \frac{500}{40} = 12.5 \approx 13$$

Area of lavatory:

$$S_{lav} = 1.5\ (m^2)$$

Lavatory width:

$$b_{lav} = 1\ (m)$$

The design of the toilet is similar to the prototype aircraft.

1.3.6. Layout and calculation of basic parameters of tail unit

The main criterion for tail design is to provide adequate stability and maneuverability for the aircraft. Mechanically, this can be understood as providing sufficient moment around the aircraft's center of gravity that can counteract the destabilizing forces of the aircraft geometry.

Range of static moment coefficients A_{HTU} and A_{VTU} are given in the table.

Determination of the tail unit geometrical parameters

In the first step, the length of horizontal tail unit is obtained:

$$L_{HTU} \approx L_{VTU} = 3.3 \cdot 8.98 = 29.6\ (m)$$

Area of horizontal tail unit is equal:

$$S_{HTU} = \frac{b_{MAC} \cdot S_w}{L_{HTU}} \cdot A_{HTU} = \frac{8.98 \cdot 489.11}{29.63} \cdot 0.65 = 96.34\ (m)$$

Area of vertical tail unit is equal:

$$S_{VTU} = \frac{l_w \cdot S_w}{L_{VTU}} \cdot A_{VTU} = \frac{60.12 \cdot 489.11}{29.63} \cdot 0.08 = 79.38\ (m)$$

where L_{HTU} and L_{VTU} - length of horizontal and vertical empennage, l_w and S_w - wingspan and area of the wing, A_{HTU} and A_{VTU} - coefficients of static moments.

Determination of the elevator area and rudder area:

Elevator area:

$$S_{el} = 0.275 \cdot S_{HTU} = 0.275 \cdot 96.34 = 26.5\ (m^2)$$

Rudder area:

$$S_{rud} = 0.33 \cdot S_{VTU} = 0.33 \cdot 79.384 = 26.2\ (m^2)$$

Selection of the area of aerodynamic balance:

If the speed of the flight $M \geq 0.75$, then:

$$S_{abea} \approx S_{abed} = 0.18..0.2 \cdot S_e$$

To prevent over balance of the control surface we need to consider:

$$\frac{S_{abea}}{S_{ea}} = \frac{S_{abed}}{S_{ed}} \leq 0.3$$

Elevator balance area is equal:

$$S_{eb} = 0.2 \cdot S_{el} = 0.2 \cdot 26.5 = 5.3\ (m^2)$$

Rudder balance area is equal:

$$S_{rb} = 0.2 \cdot S_{rud} = 0.2 \cdot 26.2 = 5.24\ (m^2)$$

The area of elevator trim tab:

$$S_{te} = 0.1 \cdot S_{el} = 0.1 \cdot 26.5 = \ 2.65\ (m^2)$$

The area of rudder trim tab is equal:

$$S_{tr} = 0.08 \cdot S_{rud} = 0.08 \cdot 26.2 = \ 2.1\ (m^2)$$

Tapper ratio of horizontal and vertical tail unit we need to choose:
For planes $M < 1$ corresponds to $\eta_{HTU} = 2 \ldots 3;\ \eta_{VTU} = 1 \ldots 3.3;$
Aspect ratio of horizontal and vertical tail unit we may recommend:
For subsonic planes $\lambda_{HTU} = 0.8 \ldots 1.5;\ \lambda_{VTU} = 3.5 \ldots 4.5;$
Root chord of horizontal stabilizer is:

$$b_{oHTU} = \frac{2 \cdot S_{HTU} \cdot \eta_{HTU}}{(\eta_{HTU} + 1) \cdot l_{HTU}} = \frac{2 \cdot 96.34 \cdot 2.63}{(2.63 + 1) \cdot 21.3} = 6.56\ (m)$$

$$l_{HTU} = 0.354 \cdot l_w = 0.354 \cdot 60.12 = 21.28\ (m)$$

Tip chord of horizontal stabilizer is:

$$b_{tHTU} = \frac{b_{oHTU}}{\eta_{HTU}} = \frac{6.56}{2.63} = 2.5\ (m)$$

Root chord of vertical stabilizer is:

$$b_{oVTU} = \frac{2 \cdot S_{VTU} \cdot \eta_{VTU}}{(\eta_{VTU} + 1) \cdot l_{VTU}} = \frac{2 \cdot 79.4 \cdot 3.1}{(3.1 + 1) \cdot 10.35} = 11.6\ (m)$$

$$l_{VTU} = 0.1722 \cdot l_w = 0.1722 \cdot 60.121 = 10.35\ (m)$$

Tip chord of vertical stabilizer is:

$$b_{tVTU} = \frac{b_{oVTU}}{\eta_{VTU}} = \frac{11.6}{3.1} = 3.74\ (m)$$

The sweepback angle of the empennage is taken as 3...50˚ more than the sweepback of the wing.

So: $\chi_{HTU} = 35$ ˚; $\chi_{VTU} = 45$ ˚.

1.3.7. Landing gear design

One of the main moving parts on an aircraft is the landing gear. It must provide good riding power during taxiing and safely absorb energy during landing. It also provides stability and maneuverability for the aircraft while on the ground by rationalizing all parameters. In the preliminary design phase, only some of the important parameters can be determined.

Main wheel axel offset is:

$$B_m = 0.23 \cdot b_{MAC} = 0.23 \cdot 8.98 = 2.07\ (m)$$

Landing gear wheel base can be estimated by:

$$B = 0.41 \cdot l_f = 0.41 \cdot 70 = \ 28.8\ (m)$$

Front wheel axial offset will be equal:

$$B_n = B - B_m = 28.8 - 2.0654 = \ 23.74\ (m)$$

Wheel track is:

$$T = 0.4 \cdot B = 0.4 \cdot 28.8 = 11.52\ (m)$$

The size, type and pressure of the landing gear tires depend on the takeoff weight of the aircraft, the dynamic loads on takeoff and landing and the condition of the runway surface.

The load on the wheel is estimated as follows:

Kg = 1.5...2.0 – dynamic coefficient.

Nose wheel load is equal:

$$P_{NLG} = \frac{B_m \cdot m_0 \cdot g \cdot K_g}{B \cdot z_{NLG}} = \frac{2.07 \cdot 322080 \cdot 9.81 \cdot 1.75}{28.8 \cdot 2} = 198267.95\ (N)$$

Main wheel load is equal:

$$P_{MLG} = \frac{\left((B - B_m) \cdot m_o \cdot g\right)}{B \cdot n_{MLG} \cdot z_{MLG}} = \frac{\left((28.8 - 2.07) \cdot 322080 \cdot 9.81\right)}{288.8 \cdot 2 \cdot 6} = 244417.7\ (N)$$

Where n and z – number of the MLG and wheels on one MLG, respectively;

Table 1.4 – Aviation tires for designed airplane

Main gear		Nose gear	
Tire size	Ply rating	Tire size	Ply rating
1246×483mm	34	1130×419 mm	28

1.3.8. Power plant

According the required takeoff thrust of the designing airplane, the following three existing engines in the market are chosen: CF6-50, CF6-80A, RB211-524G - three high bypass turbofan engine, in various modifications installed on passenger aircraft Airbus A300, Boeing 767/Airbus A310 and Boeing 747-400.

Table 1.5 – Examples of applicable engines for our designing airplane

Model	Thrust	Bypass ratio	Dry weight
CF6-50	54000 lbf (240 kN)	4.4	4104kg
CF6-80C2	56000 lbf (250 kN)	5.2	4400kg
RB211-524G	58000 lbf (260 kN)	4.3	5700 kg

After a comparative study, among the above engine variants, the CF6-50 engine is the most compliant in terms of parameters, and it is equipped with [6]:

1) a single stage fan with three low-pressure compressor (booster) stages;

2) a 14-stage, single-rotor variable-stator compressor;

3) an annular combustor;

4) a two-stage, air-cooled high pressure turbine;

5) a four-stage low pressure turbine;

6) an accessory gearbox located on the bottom of the engine fan case.

1.4. Determination of the aircraft centre of gravity position

One of the primary concerns in the design process of an aircraft is the weight distribution of the aircraft. The weight distribution of an aircraft is closely related to the performance and airworthiness of the aircraft. At one time, aircraft design must always consider the impact of each design decision and choice on the weight distribution of the aircraft. Two parameters related to aircraft weight distribution affect airworthiness and performance: 1) the aircraft center of gravity and 2) the aircraft mass moment of inertia.

The center of gravity is the point of action of the combined forces of gravity on the object, in layman's terms, the point at which it is suspended and can be balanced. The center of gravity of the aircraft is the core parameter for analyzing and evaluating the stability and controllability of the aircraft. All calculations are based on this position, especially the calculation of the aerodynamically generated moments. The calculation of the center of gravity position is therefore a crucial step in the aircraft design process. During the aircraft design process, the center of gravity of the aircraft must be placed in an ideal range under different loading conditions through the proper placement of the components. The center of gravity of an aircraft can be calculated by simply dividing the sum of the moments of gravity on each part of the aircraft with respect to the nose and the total weight.

The distance between the front and rear center of gravity is called the center of gravity range. During flight, the center of gravity must remain within that range as fuel and supplies are consumed. This center of gravity range depends primarily on the Mach number. The rear center of gravity affects mainly the longitudinal and directional stability of the aircraft, while the front center of gravity affects mainly the longitudinal and directional controllability of the aircraft. The range of the forward and aft center of gravity also affects the size of the horizontal and vertical tail and the geometry of the elevator and rudder on which they are mounted.

There are two main aspects of the weight distribution of an aircraft: 1) the internal situation such as the arrangement of seats and the location of various

facilities and equipment; and 2) the external situation such as the installation position of the wings, engines and tail units. In practice, it is very difficult to meet all these requirements perfectly, because many of them contradict each other, so only the best possible solution can be found.

The aircraft must be stable, controllable and safe in all possible center of gravity situations when flying within the flight envelope. If the over-center of gravity is too far forward, the aircraft will have difficulty overcoming gravity and climbing during takeoff, requiring a longer time and runway length. The angle of climb and maximum lift are reduced, thus the range is affected and shortened. The speed of landing will also be faster. If the aircraft's center of gravity is behind the main landing gear, the aircraft is likely to be nose up and the tail will collide with the ground.

As mentioned above, the determination of the aircraft's center of gravity is the parameter that has the greatest impact on the aircraft in projected stages. In order to facilitate the analysis, the following calculation of the center of gravity is divided into three steps: the calculation of the center of gravity of the equipped wing, the calculation of the center of gravity of the equipped fuselage, and the calculation of the center of gravity of the whole aircraft by combining the two.

1.4.1. Determination of centering of the equipped wing

The mass of the wing itself, the mass of the equipment mounted in the wing, and the mass of the fuel together make up the equipped wing. The main landing gears and the nose landing gear are also included in the trim sheet of the equipped wing. The trim sheet includes object names, mass and the center of gravity coordinate of the corresponding component. The origin of the corresponding coordinate system is the projection point of the foremost part of the aircraft mean aerodynamic chord on the fuselage. A positive value means that the center of gravity coordinate of the component is behind the origin.

The list of the mass statistic for the wing, with engines mounted under the wing, are shown in the Table 1.5. The maximum take off mass of aircraft is 322080 kg.

Since the designed aircraft is symmetrical with respect to the vertical axis, the position of the center of gravity must lie on the vertical axis, and what needs to be determined are its coordinates on the vertical axis. Coordinates of the center of gravity for the equipped wing can be calculated by:

$$x_w^{'} = \frac{\sum m_i \cdot x_i^{'}}{\sum m_i}$$

Table 1.5 - Trim sheet of equipped wing masses

№	Object name	Mass		C.G. coordinate, $x_i^{'}\,(m)$	Moment of mass $(kg \cdot m)$
		Units	Total mass, $m_i\,(kg)$		
1.	Wing (structure)	0.09477	30523.52	3.7716	115122.5
2.	Fuel system	0.0129	4154.8	3.7716	15670.4
3.	Flight control system, 30%	0.0012	386.5	5.388	2082.44
4.	Electrical equipment, 10%	0.0029	673.15	0.898	604.5
5.	Anti-ice system, 50%	0.00985	3172.5	0.898	2848.9
6.	Hydraulic system, 70%	0.00889	2863.3	5.388	15427.4
7.	Inboard engines*2	0.04275	13768.9	-1.671	-23007.87
8.	Outboard engines*2	0.04275	13768.9	3.848	52982.8
	Equipped wing without landing gear and fuel	0.21601	69311.62	2.622	1.81731
9.	Nose landing gear	0.0041822	1347	-24.31	-32745.65
10.	Main landing gear	0.0338378	10898.5	4.49	48934.17
11.	Fuel	0.3821	123066.8	3.7716	464158.6
Total		0.63532	204623.9	3.24	662078.8

$$x_w^{'} = \frac{\sum m_i \cdot x_i^{'}}{\sum m_i} = \frac{662078.8}{204623.9} = 3.24\,(m)$$

1.4.2. Determination of centering of the equipped fuselage

The origin of the coordinate system is defined as the foremost point of the aircraft's fuselage. The list of mass statistic for the fuselage are shown in table 1.4.2.

The coordinate of center of gravity of the equipped fuselage cam be obtained as follows:

$$x_f = \frac{\sum m_i \cdot x_i}{\sum m_i}$$

where x_i – center of gravity coordinate of objects on the aircraft; $\sum m_i$ – sum of total mass of fuselage.

Table 1.6. – Trim sheet of equipped fuselage masses

№	Objects names	Mass		C.G. coordinates, $x_i\ (m)$	Moment of mass, $(kg \cdot m)$
		Units	Total mass, $m_i\ (kg)$		
1	2	3	4	5	6
1.	Fuselage	0.07462	24033.61	35	841176.4
2.	Horizontal tail	0.00982	3162.8	67.06	212106
3.	Vertical tail	0.01014	3265.9	65.08	212568.4
4.	Radar	0.0018	579.75	0.6	347.85
5.	Radio equipment	0.0013	418.7	2.5	1046.8
6.	Instrument panel	0.0031	998.45	2.5	2496
7.	Navigation equipment	0.0027	869.62	2.5	2174
8.	Aircraft control system, 70%	0.0028	901.8	35	31563.8
9.	Hydraulic system, 30%	0.00381	1227.1	42	51539.25
10.	Anti ice system, 25%	0.004925	1586.25	21	33311.1
11.	Air conditioning system, 25%	0.004925	1586.25	35	55518.5

1	2	3	4	5	6
12.	Electrical equipment, 90%	0.01881	6058.325	35	212041.4
13.	Lining and insulation	0.0061	1964.7	35	68764
14.	Not typical equipment	0.00162	521.77	35	18261.98
15.	Additional equipment	0.00748	2409.16	35	84320.55
16.	Operational items	0.01829	5890.85	35	206179.5
	Furnishings:	0.0177	5700.8		
17.	Lavatory, 40%		2280.33	34.2	77972.6
18.	Galley, 60%		3420.49	31.5	107621.4
	Passenger equipment	0.0125	4026		
19.	Passenger seats		3500	31.75	111109.7
20.	Seats of light attendants		70	35	2450
21.	Seats of pilots		456	2	912
	Equipped fuselage without payload		65201.87	35.8	2333481.4
	Payload	0.16223	52251		
22.	On board meal		412	31.5	12963
23.	Baggage, cargo, mail		12871.7	32.06	388881.3
24.	Passengers		38555.35	31.8	1223964
25.	crew		412	2	824
	Total	0.36467	117452.9	33.9	3984019.6
	Total fraction	0.99999			

We can find fuselage center of gravity coordinate x_f :

$$x_f = \frac{\sum m_i \cdot x_i}{\sum m_i} = 33.92\ (m)$$

After we determined the center of gravity of fully equipped wing and fuselage, we construct the moment equilibrium equation relatively fuselage nose:

$$m_f \cdot x_f + m_w(X_{MAC} + x_w^{'}) = m_0 \cdot (X_{MAC} + C)$$

where m_0 – aircraft takeoff mass, kg; m_f – mass of equipped fuselage, kg; m_w – mass of equipped wing, kg; C – distance from mean aerodynamic chord leading edge to the center of gravity point, determined by the designer. C = (0.23...0.32) b_{MAC} – high wing;

Then, the distance between the foremost part of the mean aerodynamic chord and the foremost part of the fuselage nose can be obtained by the following formula:

$$X_{MAC} = \frac{m_f \cdot x_f + m_w \cdot x_w^{'} - m_0 \cdot C}{m_0 - m_w}$$

$$= \frac{3984019.6 + 662078.2 - 322080 \cdot 2.5144}{322080 - 204623.9} \approx 32.66\ (m)$$

$$X_c = \frac{X_{c.g.} - X_{MAC}}{b_{MAC}} \cdot 100\%$$

Table 1.7.- Calculation of center of gravity positioning variants

Object name	Mass, (kg)	Coordinate, (m)	Mass moment, ($kg \cdot m$)
Equipped wing (without fuel and landing gear)	69311.6	35.28	2445532.5
Nose landing gear (extended)	1347	8.35	11249.11
Main landing gear (extended)	10898.5	37.15	404891.7
Fuel/fuel reserve	123066.77	36.43	4483668.56
Equipped fuselage (without payload)	65201.87	35.79	2333481.37
Passengers of economy class	38555.35	31.75	1223964.11
Baggage, cargo and mail	13283.7	32.07	425999.6
Crew	412	2	824
Nose landing gear (retracted)	1347	7.35	9902.16
Main landing gear (retracted)	10898.5	37.15	404891.7
Reserve fuel	11759.14	36.43	428418.6

Table 1.8. - Airplanes center of gravity position variants

Variants of loading	Mass (kg)	Mass moment (kg·m)	Center of mass (m)	Centering
Take off mass (L.G. extended)	322076.79	11329611	35.17674	0.28
Take off mass (L.G. retracted)	322076.79	11328264	35.17255	0.2796
Landing weight (LG extended)	210769.16	7274361.02	34.5	0.206
Ferry version	270237.75	9679647.27	35.82	0.35
Parking version	146758.97	5195154.7	35.4	0.305

1.5. Conclusions for the project part

By analyzing the calculated data of the designed aircraft, it is possible to obtain that the designed aircraft fully meets the design expectations and requirements, just like the prototype Boeing 777, with high transportation efficiency and a comfortable and safe environment for passengers.

In the first part of this paper, the main parameters of the main components of the aircraft, such as wings, fuselage, tail plane, landing gear, engines, etc., are studied and selected. After the design of the main parts of the aircraft, such as the wings and fuselage, the calculation of the center of gravity of the equipped aircraft is also performed. After detailed calculation, it can be seen that the center of gravity of the designed aircraft is in the range of 0.20 to 0.35 for five different load cases, which meets the safety requirement of the aircraft to be reached.

PART 2

FLOOR PANEL DESIGN

2.1. Statement on the topic

A sandwich panel structure is a regular, ordered, ultra-light porous material with high specific stiffness, ultra-lightweight, and high specific surface area. The structure has the advantages that the traditional stiffened plates cannot match in terms of acoustics, and fatigue and impact resistance, and thus has become an important material in aircraft structural design [7]. As part of the aircraft structure, the aircraft floor not only provides a platform for passengers and cargo to walk and slide on, but also plays an important role in the safety of the aircraft during normal operations, emergency landings and emergency decompression. Therefore, there is no doubt that the analysis of aircraft floor strength is an integral part of the aircraft manufacturing process.

2.2. Introduction to sandwich structure

Of all the available design concepts for composite structures, sandwich structures are becoming increasingly important due to the continued development of man-made honeycomb materials as a core material. A structural sandwich is a special form of a laminated composite comprising of a combination of different materials that are bonded to each other so as to utilize the properties of each separate component to the structural advantage of the whole assembly[8].

The sandwich structure consists of two thin high-strength face sheets, a core that separates the two face sheets and transfers the load from one face sheet to the other, and an adhesive material that is capable of transferring shear loads and axial loads from and to the core (Fig. 2.1). Sandwich construction works in much the

same way as an I-beam, which is an effective structural shape because the vast majority of materials are used on the flanges away from the neutral axis, only a small amount of sufficient material is used on the web that connects the upper and lower flanges, and the web plays the role of resisting shear and buckling and linking the upper and lower flanges, so the material of the I-beam is used very efficiently. In sandwich construction, the face sheet acts as the flange and the core acts as the web. Unlike the web material of I-beam, which is concentrated in a narrow strip on the flange, the core material of sandwich structure is distributed over the whole sheet, thus forming a continuous support for face sheets, and because the sandwich structure is not integrally formed, face sheets and cores can be made of different materials according to their different stress characteristics. The upper and lower face sheet will work together to create an efficient stress couple or resisting moment to counteract the bending moment applied to the exterior. The core resists shear forces and stabilizes the panels against bending or wrinkling [9]. As for the types of sandwich components considered in this paper, the face sheets is composed of thin, high strength materials, while the core material is light weight and thick, but with relatively low strength. The selection of the materials that make up each component depends primarily on the specific application of the sandwich panel and the criteria associated with it.

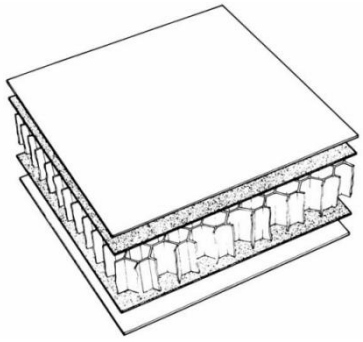

Fig 2.1. Sandwich structure with honeycomb core

Sandwich construction allows for efficient design to maximize the use of components and materials. The greatest advantage of this structure is the very high stiffness-to-weight ratio and bending strength-to-weight ratio. The ability of sandwich panels to increase flexural stiffness significantly without a significant increase in weight makes this structure preferable to conventional structures. With little increase in weight, the upper and lower face sheets separated by the core increase the moment of inertia of the panel, producing an effective bending resistant structure, an effective structure to resist bending and buckling loads. Table 2.1 shows illustratively the flexural stiffness and strength advantage of sandwich panels compared to solid panels using typical beam theory with typical values for skin and core density. By splitting a solid laminate down the middle and separating the two halves with a core material, the result is a sandwich panel. The new panel weighs little more than the laminate, but its flexural stiffness and strength is much greater; by doubling the thickness of the core material, the difference is even more striking [10]. As mentioned above, different from I-beam structures, the continuous support of face sheets by the core allows the sheets to remain flat without buckling when subjected to high compression forces. This is important for aircraft structures because the aircraft floor needs to remain flat under load in order to give a smooth platform for the people on board as well as the cargo. Sandwich constructions also exhibit superior insulation. In some deformation modes, the absorption of mechanical energy can be increased exponentially compared to monocoque structures due to the imposed shorter buckling wave modes [11]. Due to the natural characteristics of this structure, thermal conductivity is very poor, so there is no need to use additional insulation materials, thus maintaining the light weight of the sandwich structure. Sandwich panels can be manufactured in one large whole piece, providing a large smooth area as no connections such as rivets and bolts are required. This means that fewer parts are required and the assembly of the structure is simplified, the reduced number of weld seams and the high stiffness

of the panels both reduce weld distortion. Due to the high stiffness of the sandwich structure, the frame spacing can be increased, which further reduces the weight of the structure and resulting in cost savings and thus a smooth and continuous load pattern without causing stress concentrations.

Table 2.1. Influence of core thickness on panel weight and bending performance [10].

			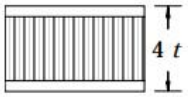
Relative Bending Stiffness	1	7.0	37
Relative Bending Strength	1	3.5	9.2
Relative Weight	1	1.03	1.06

2.3. Honeycomb cores

The basic cell shapes are the hexagon, square and flex core. Some of the variations of these shapes are the overexpanded, underexpanded and reinforced. Figure 2.2 shows all of these configurations [12]. The most common shape is the hexagon owing to the advantages they offer in manufacturing. Among these shapes, over-expanded hexagonal and flexible core are mainly used in cases where bending of the core is required in the manufacturing process of sandwich structures. These two shapes reduce the anti-elastic bending and cell wall buckling during bending. Other cell shapes such as rectangular and reinforced hexagonal are also available.

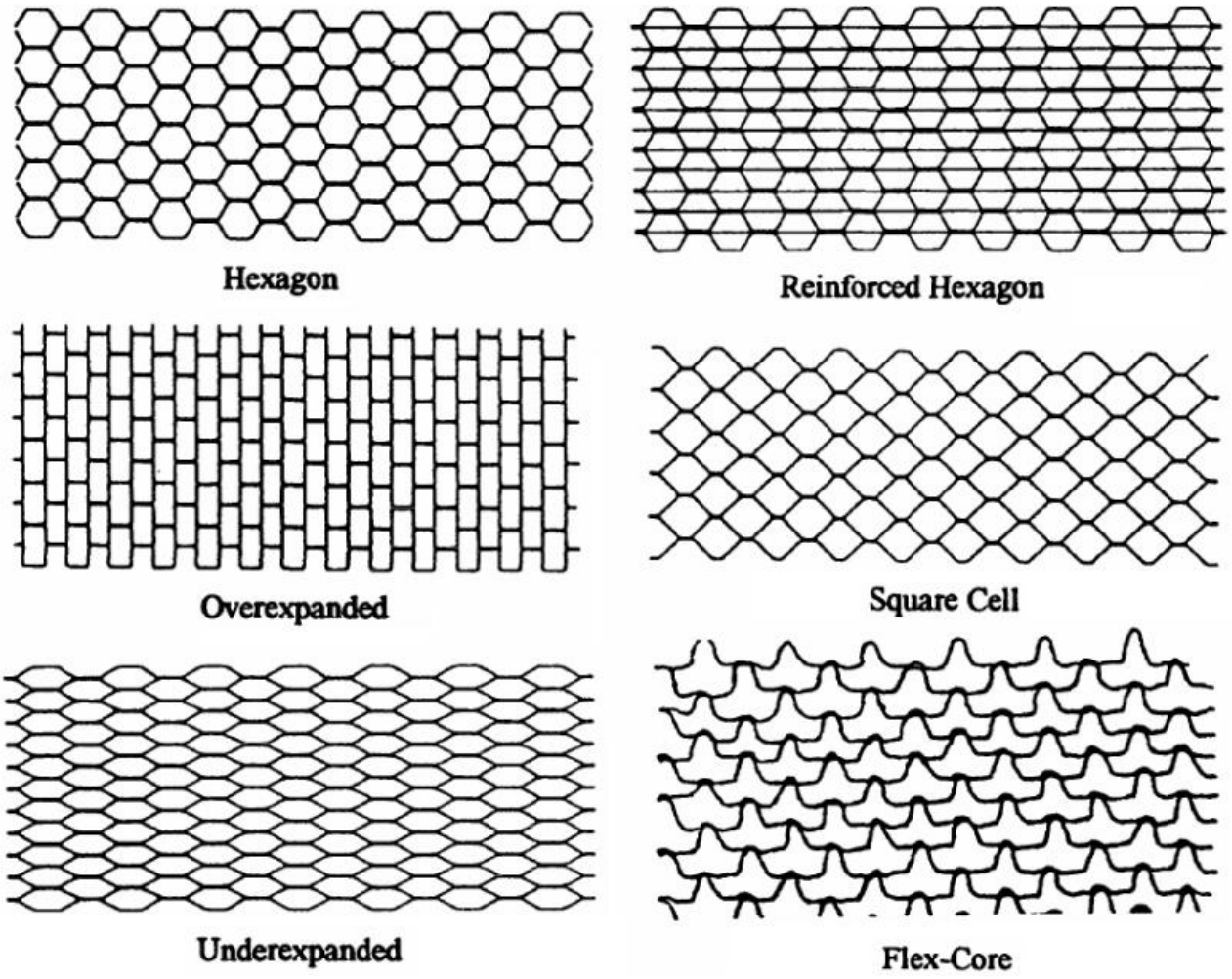

Fig 2.2. Most commonly used cell shapes for honeycomb core materials

Due to the manufacturing methods, most honeycomb materials have both different out-of-plane properties and in-plane properties. Because either the corrugation process or the expansion process will produce a double cell walls in one orientation and single cell walls in the other orientation as a result of bonding two pieces of aluminum together, the double cell wall direction is known as the "ribbon" or "L" direction, as shown in Figure 2.3. The over-expanded cell shape creates additional anisotropy because it is not a positive hexagon [9]. The material properties of most honeycomb materials have three main directions: *W* (width), *L* (length or ribbon) and *T* (thickness) directions (Fig 2.3).

There are two principal methods of converting sheets into honeycomb materials in the case of aluminum manufacturing (Fig 2.4). The expansion

process begins by stacking sheets of aluminum of appropriate thickness with adhesive nodes printed on them. This stacking of multiple sheets makes a block. The block is then cut in the T-direction or thickness direction to the specified thickness. Once the adhesive has cured, the block is stretched in the W direction or width direction until the desired hexagonal shape is achieved.

The corrugation process is to feed a roll of aluminum sheet through a corrugated roller to form pre-corrugated sheets. An adhesive is applied to the flat portions of these sheets and then the pre-corrugated sheets are stacked together into blocks. Once the adhesive has cured, the specified thickness of blocks can be cut out of the stack. This is typically done for honeycomb cores with smaller cell sizes than those made by the expansion process.

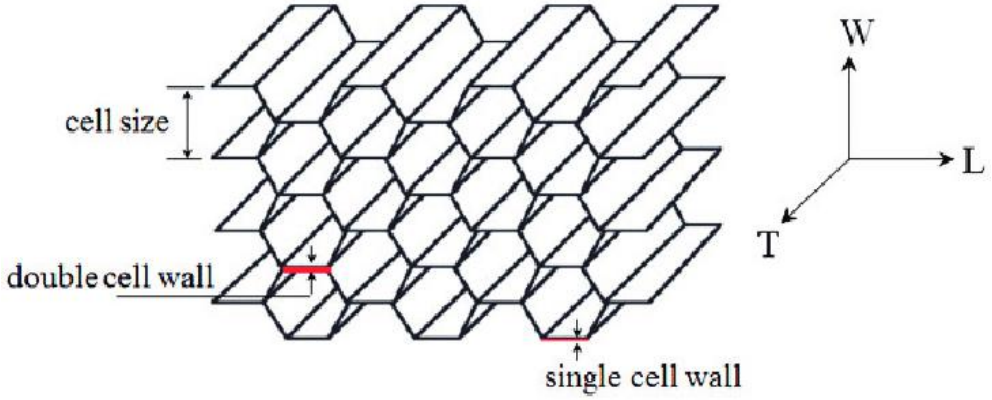

Fig 2.3. Three main directions of honeycomb material

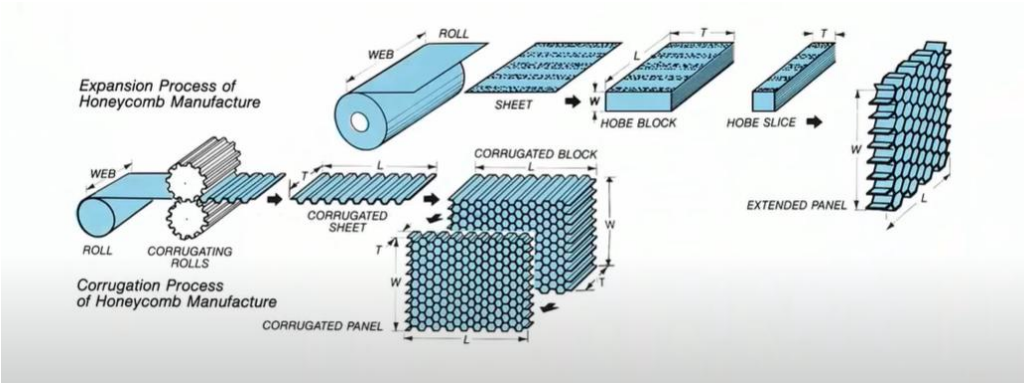

Fig 2.4. Two principal methods of honeycomb manufacturing

2.4. The properties of aluminum sandwich structure

Aluminum sandwich structure is a widely used structure in the design of structures in the field of lightweight transportation, where aircraft are in the field. The purpose of this paper is to theoretically analysis the strength performance of aluminum sandwich panel.

Before studying and designing aluminum sandwich panels, it is necessary to first define the notation for the basic geometric characteristics. The honeycomb sandwich panel considered in the paper is shown in the Figure 2.5. To simplify the analysis process, and according to the general application of sandwich panels, the thickness of the top and bottom face sheets t_f should be assumed to be the same. The core height is defined as h_c.

For the analysis purpose, one unit of honeycomb core is defined in the Figure 2.6 below, and the W and L directions are in the directions perpendicular and parallel to the double cell walls of the honeycomb core of the sandwich panel, respectively.

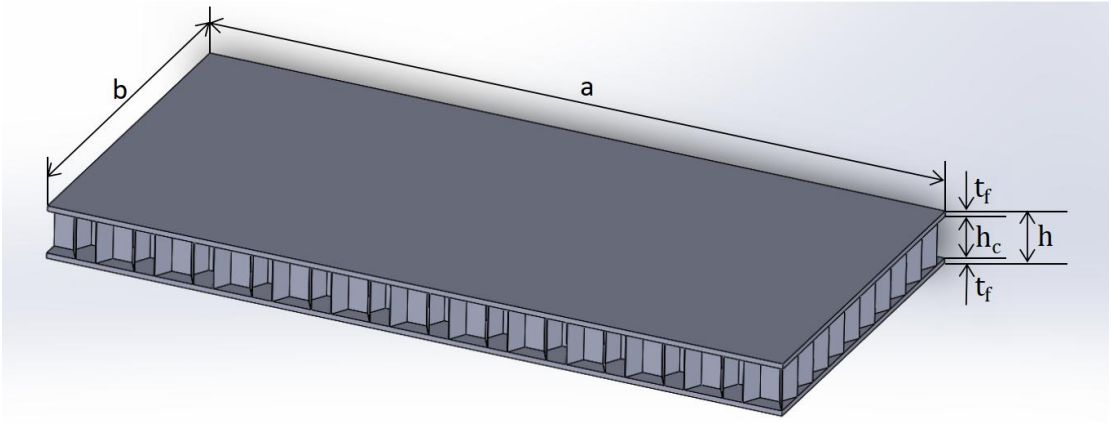

Fig 2.5. Honeycomb core sandwich panel

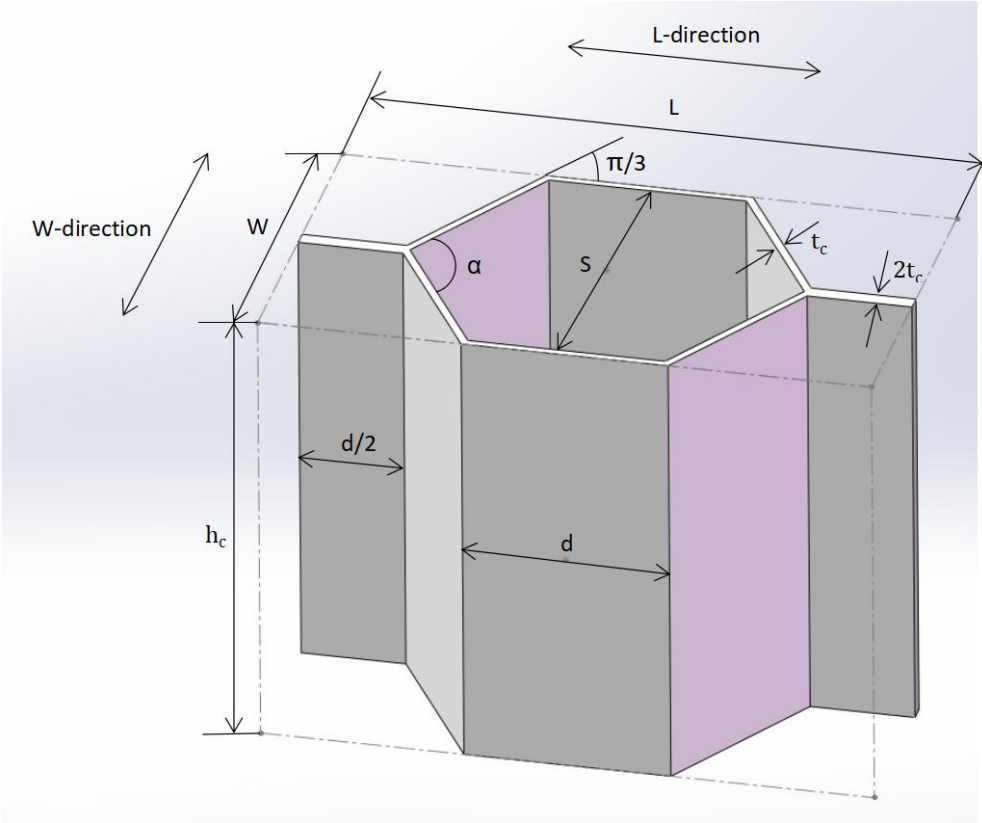

Fig 2.6. A unit honeycomb core

As mentioned above, the face sheets of the sandwich panel can be considered as the flanges of an I-beam, because most of the bending stresses on sandwich panels are borne by them, in general, the upper face sheet is in compression and the lower face sheet is in tension. Similarly, the core material is similar to the web in I-beam, so it can be assumed that the core material is only subjected to shear and not to longitudinal stress. The core separates the top and bottom face sheets by its thickness much greater than that of the face sheets, thus increasing the stiffness of the structure. The core material and the face sheets are rigidly connected by adhesives and other joining methods, so that the components are combined into one piece and have high torsional and bending stiffness.

After determining the notations of each geometric characteristic, the next step is to determine the specific geometric parameters and the mechanical properties of each component of the sandwich panel to be studied in this paper.

Material selection based on Collins Aerospace's aeroMETAL™ Honeycomb Panels [13]. The sandwich panel to be studied in this paper consists of two materials, 5052 aluminum alloy for honeycomb cores and 2024-T3 clad aluminum alloy for face sheets.

Mechanical properties of face sheets material 2024-T3 are presented in the Table 2.2 below [14].

Table 2.2. mechanical properties of face sheets material 2024-T3

Young's modulus, E_f (MPa)	73100
Yield strength, σ_{fo} (MPa)	290
Tensile strength (MPa)	435
Elongation at break (%)	12
Density, ρ_f (g/cm^3)	2.78

Mechanical properties of aluminum honeycomb core material 5052 are presented in the Table 2.3 below [15].

Table 2.3. Mechanical properties of aluminum honeycomb core material 5052

Item	Core density, ρ_{core} (69 kg/m^3)
0.2% yield strength, σ_{co}(MPa)	193
Young's modulus, E_c (MPa)	70300
Compressive strength (MPa)	4.2
Compressive modulus (MPa)	401
Shear modulus, G_{cL} (MPa)	41400
Shear modulus, G_{cW} (MPa)	26500
Poisson ratio, v_c	0.33

In order to meet the actual needs, according to the 508mm frame pitch of the prototype Boeing 777 [16], the distance between the seat rail of the designed aircraft 550mm and the data from the Aluminum Honeycomb Core -5052 supplied by CT-Sim GmbH [17], the geometric parameters of the sandwich plate to be studied in this paper are defined in the following table.

Table 2.4. Dimensions of the sandwich panel

Item	Property	Value
Panel	Length (mm): a	550
	Width (mm): b	508
	Height (mm): h	10
Core	Cell size (mm): S	6.35
	Thickness (mm): t_c	0.05
	Height (mm): h_c	8
Face sheets	Thickness (mm): t_f	1

The second axial moment of area of the honeycomb sandwich panel can be calculated by the following formula

$$I_f = \frac{(h^3 - h_c^3) \cdot b}{12} = \frac{(10^3 - 8^3) \cdot 508}{12} = 20658.67\ (mm^4)$$

The virtual area of a unit honeycomb core in the plane parallel to the plane where face sheets are located can be calculated by

$$A = W \cdot L = 6.35 \cdot 11 = 69.84\ (mm^2)$$

One of the most important reasons why aluminum honeycomb materials are widely used is their light weight. Therefore, it is important to accurately calculate

the weight of aluminum honeycomb sandwich panels in order to correctly compute the performance of sandwich structures, such as the strength to weight ratio. The mass of the aluminum sandwich panel can be obtained from

$$m = m_c + m_f = \rho_{core} \cdot V_c + \rho_f \cdot V_f$$
$$= \frac{550 \cdot 508 \cdot 8 \cdot 0.069}{1000} + \frac{2 \cdot 550 \cdot 508 \cdot 1 \cdot 2.78}{1000} = 1707.7\ (g)$$

In each honeycomb cell, there are two double cell walls of $2t_c$ thickness (two cell walls of t_c thickness combined with each other), and four single cell walls of t_c thickness. When calculating the wall cross-sectional area A_w of the cell, only half of the cell wall thickness is used, since each cell wall plate is naturally shared by two neighboring cells. That is, for separate cell walls, thickness $\frac{t_c}{2}$ is used, and for bonded double walls, thickness t_c is used.

The cross-sectional area of the A_w of the unit cell wall, consisting of two bonded surfaces and four free surfaces, can be calculated by

$$A_w = 2d \cdot \frac{2t_c}{2} + 4d \cdot \frac{t_c}{2} = 4dt_c$$

The cross-sectional area of a unit hexagonal cell (consisting of 6 equilateral triangles) can be calculated as

$$A_c = 6 \cdot \frac{\sqrt{3}d^2}{4} = \frac{3\sqrt{3}d^2}{2}$$

From the above equation, the average density of the honeycomb core can be expressed as

$$\frac{\rho_{cm}}{\rho_c} = \frac{A_w}{A_c}$$

So, after ignoring the portion of the core weight accounted for by the adhesive and other materials used to adhere the two cell walls, we can estimate the average density of the honeycomb core (without adhesive) by the following formula

$$\rho_{cm} = \frac{8t_c d\rho_c}{A} \approx \frac{8t_c\rho_c}{3\sqrt{3}d} = \frac{8 \cdot 0.05 \cdot 2.78}{3\sqrt{3} \cdot 3.666} = 58.37\ (kg/m^3)$$

Since the formula is the geometric parameters of the honeycomb cell and the density of the aluminum used in the core, this average density is a practical parameter to calculate the performance of the honeycomb core.

2.5. Theoretical analysis of the present sandwich panel

The prerequisite for the rational design of structures in engineering design is to know the mechanical properties of the components, so the mechanical properties of sandwich structures need to be calculated quickly and accurately, which requires the simplification methods mentioned below.

2.5.1. Bending performance

A simplified method can be used to analyze the bending properties of the sandwich panels in this paper. The test commonly used to test the bending performance of a plate is the three-point bending test (Fig 2.7), suppose the sandwich panel is simply supported on two support points at a certain distance, and a downward line load is applied to the specimen along the width direction above the midpoint of the two support points, and three-point bending occurs when the three contact points of the specimen form two equal moments.

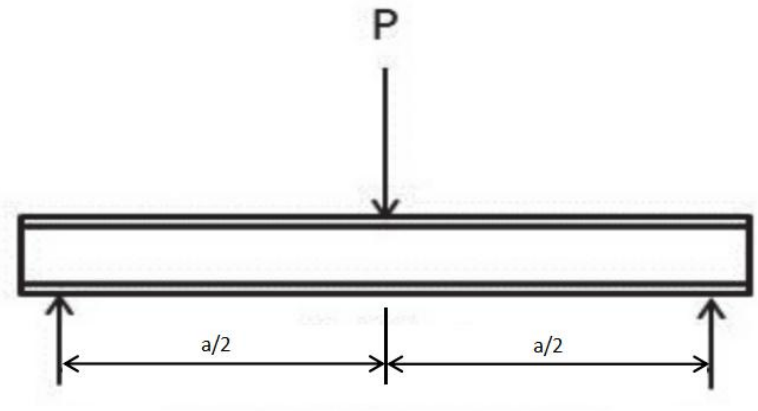

Fig 2.7 Three point mid-span loading

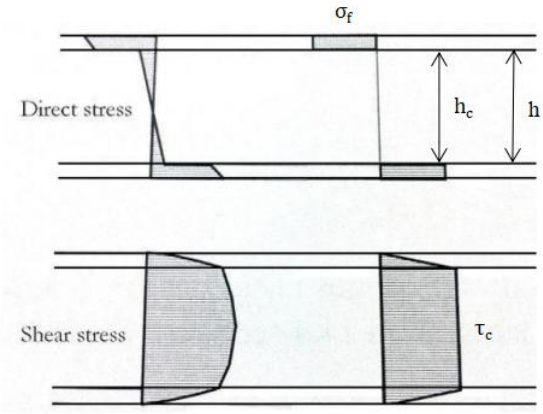

Fig 2.8 simplified distributions of direct and shear stresses in a sandwich panel

Since the principle of sandwich plate is similar to that of I-beam, for the purpose of calculation, it is assumed that face sheets are subjected to only direct stresses σ_f and honeycomb core materials are subjected to only shear stress τ_c, and because the thickness of the face sheets is relatively small compared to the panel, it is assumed that the direct stresses in the cross-section of the face sheets thickness direction are equal everywhere, and considering that the shear stresses in the core material do not vary much in the thickness direction, it is also assumed that they are equal everywhere.

There is also a simplified formula for predicting the critical value of applied loads. When the stress distribution is consistent with the Figure 2.8, the bending moment of the simply supported honeycomb sandwich beam can be estimated by

substituting the static moment of the direct stresses relative to the neutral axis of the cross-section by the following formula

$$M = \frac{Pa}{4} = C \cdot \frac{bh^2\sigma_f}{4} \cdot \left[1 - \left(\frac{h_c}{h}\right)^2\right]$$

where C is a constant related to the shear effect of the core material due to resistance to bending moment.

Assuming that the shear effect of the core on the panel strength may be similar to the shear effect of the panel stiffness, the constant C can be calculated by

$$C = \frac{C_1}{C_1 + C_2} = \frac{\frac{a^3}{48E_fI_f}}{\frac{a^3}{48E_fI_f} + \frac{a}{4A_tG_{cm}}}$$

$$= \frac{\frac{550^3}{48 \cdot 73100 \cdot 20658.67}}{\frac{550^3}{48 \cdot 73100 \cdot 20658.67} + \frac{550}{4 \cdot 508 \cdot 8 \cdot 33950}} = 0.999566$$

Where, cross sectional area of honeycomb core in the T direction $A_t = b \cdot h_c$, mean value of shear modulus of the honeycomb core $G_{cm} = \frac{G_{cL}+G_{cW}}{2}$. C_1 in the above equation is a parameter related to the bending effect only, and C_2 is due to the shear effect.

When the direct stress of the face sheets reaches the yield stress, i.e., $\sigma_f = \sigma_{fo}$, the load at this point is the critical load. Therefore, by replacing P with P_o, the equation of critical load can be derived from the above equation as follows

$$P_o = C \cdot \frac{bh^2\sigma_{fo}}{a} \cdot \left[1 - \left(\frac{h_c}{h}\right)^2\right] = 0.999566 \cdot \frac{508 \cdot 10^2 \cdot 290}{550} \cdot \left[1 - \left(\frac{8}{10}\right)^2\right]$$
$$= 9.64\ (kN)$$

The strength to weight ratio can be calculated as follows

$$\lambda = \frac{P_o}{m \cdot g} = \frac{9.64 \cdot 1000}{1.7077 \cdot 9.81} = 575.44$$

A formula of the deflection at the mid-span of the sandwich beam in the linear elastic regime introduced by Kelsey et al.[18] are as follows

$$w = \frac{P_o \cdot a^3}{48E_f I_f} + \frac{P_o \cdot a}{4A_t G_{cm}} = \frac{9640 \cdot 550^3}{48 \cdot 73100 \cdot 20658.67} + \frac{9640 \cdot 550}{4 \cdot 508 \cdot 8 \cdot 33950}$$
$$= 22.1\ (mm)$$

Kobayashi et al [19] compares the results of theoretical predictions using the above equation (i.e., between load and mid-span deflection) with the experimental results under bending (Fig 2.9). The figure also compares the theoretical results ignoring shear effects. It can be seen that the above equation predicts the linear elastic bending response of the aluminum honeycomb sandwich beam very well. It is clear that the shear stress-related effects brought about by the honeycomb core cannot be neglected.

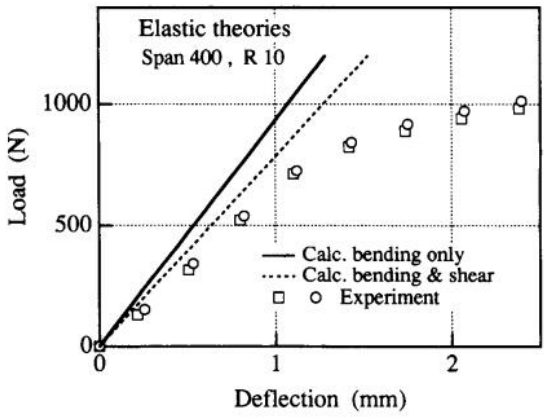

Fig 2.9 comparison of theoretical results with experimental results for three point bending test

2.5.2. Compression performance

The next step to be performed is the calculation of the ultimate strength of the honeycomb sandwich panel under compression in the length direction (Figure 2.10). We have used an equivalent single plate approach in the strength calculation, where the strength of the original honeycomb sandwich panel can be calculated by substituting the parameters of that equivalent plate. Figure 2.11 illustrates the concept of this approach.

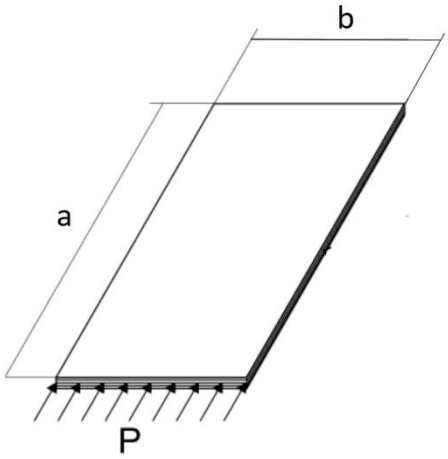

Fig 2.10 Sandwich panel under compression in the length direction

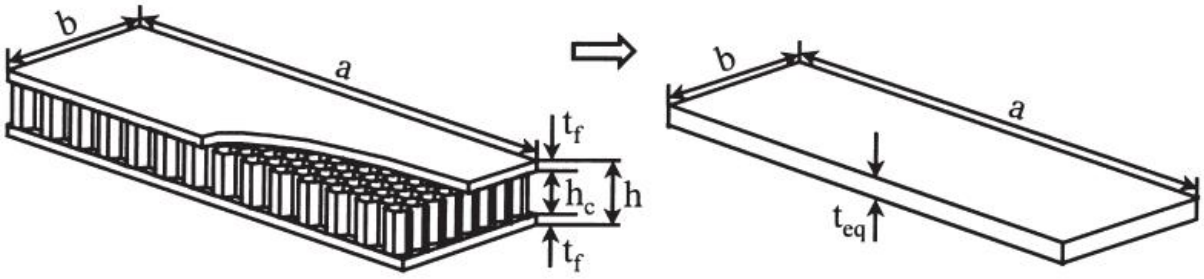

Fig 2.11 Concept of the equivalent single plate method

There are two methods of replacing a honeycomb sandwich panel with an equivalent single plate, the equivalent rigidity approach and the equivalent weight

approach. The former method decides the thickness and modulus of elasticity of the panel to make the rigidity of the sandwich panel equal to the rigidity of the single plate. The latter is done by deciding the dimensions of the equivalent single plate in order to make the structural weight of the two objects equal [20].

The equivalent rigidity method tends to have a large prediction of ultimate strength, while the equivalent weight method tends to have a small prediction of ultimate strength. The former is applicable to the case where the core material is relatively thick, while the latter is applicable to the case where the core material is relatively thin. In this paper, the core thickness of the plates is low, so the equivalent weight method is used in the following.

The equivalent plate thickness t_{eq} of the equivalent single plate can be estimated by

$$t_{eq} = \frac{2t_f\rho_f + h_c\rho_{cm}}{\rho_f} = 2.168\ (mm)$$

The elasticity and shear modulus of the equivalent single plate are approximately equal to these properties of the face sheets materials, which is

$$E_{eq} = E_f = 73100\ (MPa)$$
$$G_{eq} = G_f = 27000\ (MPa)$$

A form of the Frankland equation is then used to estimate the ultimate strength of an aluminum sandwich panel with the equivalent thickness and modulus obtained above under compression in the length direction. The equation are as follows

$$\frac{\sigma_u}{\sigma_{fo}} = 1 \quad for \quad \beta > 1$$

$$\frac{\sigma_u}{\sigma_{fo}} = \frac{a_1}{\beta} - \frac{a_2^2}{\beta^2} \quad for \quad \beta \leq 1$$

Where, $\beta = \frac{b}{t_{eq}}\sqrt{\frac{\sigma_{fo}}{E_{eq}}} = 14.75 > 1$, and a_1 and a_2 are constants related to the boundary conditions of the plate. Faulkner [21] defined that for simply supported plates, $a_1 = 2$ and $a_2 = 1$, which is the case in this paper. So the ultimate strength can be calculated by

$$\sigma_u = \sigma_{fo} = 290\ (MPa)$$

2.5.3. Crushing performance

Crushing performance is the mechanical property exhibited when a sandwich panel is subjected to impact pressure along its thickness direction as shown in Figure 2.12.

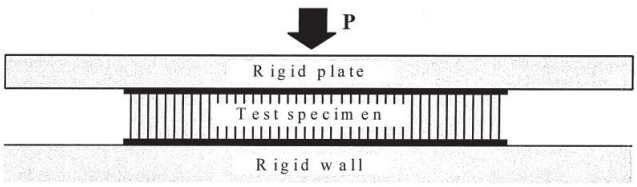

Fig 2.12 Sandwich panel under crushing test

The equation proposed by Kunimoto and Yamada [22] for estimating the maximum compressive load of a pure honeycomb core excluding face sheets under impact pressure in the thickness direction is used in the following

$$P_{uc} = 8dt_c\left[\frac{\pi^2 E_c \sigma_{co}^2 t_c^2}{3(1-v_c^2)d^2}\right]^{\frac{1}{3}} = 178.33\ (kN)$$

Wierzbicki [23] introduced the following simplified equation to estimate the mean crushing load of a pure honeycomb core excluding face sheets under crushing load, and is used below

$$P_m = 16.56A\sigma_{co} \cdot \left(\frac{t_c}{S}\right)^{\frac{5}{3}} = 71.43\ (kN)$$

Where, S is the distance between the inner edges of the two walls of a hexagonal honeycomb cell that are parallel to each other in the Figure 2.6 above.

The energy absorption capacity of a honeycomb structure depends to a large extent on its mean crushing strength. The yield strength of the pure core material and geometric parameters such as cell size and wall thickness determine this parameter. Because the density of the honeycomb is affected by the geometric parameters of the honeycomb, the crushing strength is also affected by the density.

Paik et al. [20] compared the calculated maximum and mean crushing loads with experimental results and results obtained for the bare honeycomb core by Hexcel [24] are also compared (Fig 2.13). A comparison of the maximum compressive strength of the core alone and the sandwich panel with face sheets shows that although the strength trends are very similar in both cases, there is in fact an increase in the strength of the sandwich panel with face sheets. In contrast, the experimental results without face sheets are in good agreement with those obtained by the analytical method used in this paper.

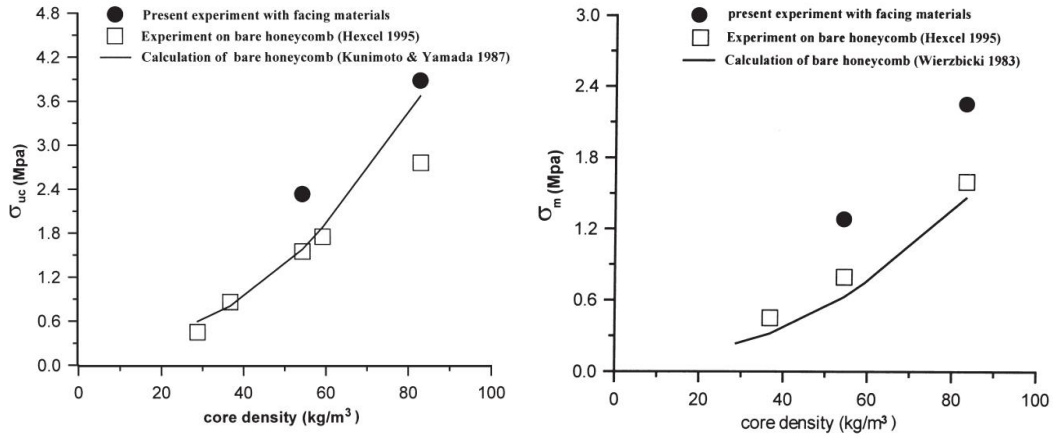

Figure 2.13 Effects of core density on the maximum compressive strength and mean crushing strength under lateral pressure.

2.6. Conclusions for the special part

In this special part, the following results are obtained:

1) The concept and working principle of sandwich panel for aircraft are investigated;

2) The different cell shapes of the core material and the two main manufacturing methods are reviewed;

3) After the geometric parameters and material selection of the sandwich plate are decided, the shape related mechanical parameters of the plate are calculated from the formula derived from the I-beam.

4) Theoretical analysis of the bending performance of the panel in the case of three-point bending. The critical load $P_o = 9.64\,kN$, this is a considerable amount of force given the dimensions and weight of the sandwich panel chosen for this paper.

5) A method of simplifying sandwich panel to the equivalent single plate to facilitate the calculation of the mechanical properties of the sandwich panel subjected to compression forces from the length direction.

6) the maximum compressive load and the mean crushing load of the sandwich panel are obtained in the case of crushing.

General conclusions

In this paper, the following results are obtained:

1) Preliminary design of a long range aircraft with a passenger capacity of 500 people;

2) Cabin layout of the long range aircraft with a passenger capacity of 500 people;

3) Four CF6-50 engines are mounted under the wings, providing high cruise speed and good thrust-to-weight ratio;

4) The center of gravity of the designed aircraft is in the range of 0.20 to 0.35 for five different load cases;

5) The features, advantages, principles and manufacturing methods of sandwich structures are introduced;

6) By reasonably selecting the dimensional parameters and materials of sandwich panels, the floor must be able to withstand loads exceeding the floor limitation of 977 kg/m^2 for the prototype aircraft Boeing 777-200ER [25] to achieve strength and comfort requirements;

7) A simplified theoretical procedure for calculating various mechanical properties of sandwich panel subjected to different loads is performed; The rationality of the calculation method and process is verified by comparing the theoretical results with the experimental results in the cited references;

References

[1] *commercial aircraft market - growth, trends, COVID-19 impact, and forecast (2021-2026)* [Digital source] - Access mode: URL: https://www.mordorintelligence.com/industry-reports/commercial aircraft-market.

[2] Chen Li, Yang Xinjun: *Status and Trends in the Development of Widebody jetliners, 2014. — 1-4 p*

[3] *Aircraft Data File* [Digital source] - Access mode: URL: https://booksite.elsevier.com/9780340741528/appendices/data-a/default.htm.

[4] Sadraey, Mohammad H: *Aircraft design: A systems engineering approach, 2012. — 220 p.*

[5] L.B. Ilcewicz, DJ. Hoffman, A.J. Fawcett: *Composite applications in commercial airframe structures, in: Comprehensive Composite Materials, 2000, — 87-119 p.*

[6] Day, Std: *C56-50A Engines, 1971. — 28 p.*

[7] Y. Hou et al.: *The bending and failure of sandwich structures with auxetic gradient cellular cores, 2013. — 119-131p.*

[8] Ramakrishnan, G., et al: *Sandwich and Natural fiber composites-A review, 2018. — 1 p.*

[9] Zenkert, Dan: *The handbook of sandwich construction, 1997. — 4 p.*

[10] Petras, Achilles: *Design of sandwich structures, 1999. — 4 p.*

[11] Vaidya, U. K., H. Mahfuz, and S. Jeelani: *Damage tolerance of resin transfer molded composite sandwich constructions, 1999. — 24 p.*

[12] Bitzer T: *Honeycomb technology: Materials, Design, Manufacturing, Applications and Testing*, 2012. — *18 p.*

[13] *aeroMETAL™ Honeycomb Panels* [Digital source] - Access mode: URL: https://www.collinsaerospace.com/what-we-do/Business-Aviation/Cabin/Structures/Honeycomb-Panels/Aerometal.

[14] *Aluminum 2024-T3* [Digital source] - Access mode: URL: http://www.matweb.com/search/DataSheet.aspx?MatGUID=57483b4d782940faaf12964a1821fb61.

[15] *Aluminum 5052* [Digital source] - Access mode: URL: http://www.matweb.com/search/datasheet_print.aspx?matguid=1a5729196f264cc78a3233bf558aee8a.

[16] *CODAMEIN - Composite Damage Metrics and Inspection (high energy blunt impact threat)* [Digital source] - Access mode: URL: https://www.easa.europa.eu/document-library/research-reports/easa20111.

[17] *Aluminum Honeycomb Core - 5052* [Digital source] - Access mode: URL: http://www.ct-sim.eu/honeycombcore/nida-aluminum-honeycomb-technical-doc-v06-en.pdf

[18] Kelsey S, Gellatly RA, Clark BW: *The shear modulus of foil honeycomb cores, 1958. — 294-308 p.*
[19] Kobayashi H, Daimaruya M, Okuto K: *Elasto-plastic bending deformation of welded honeycomb sandwich panel, 1994. — 105 p.*
[20] Paik, J.K., Anil, K., Thayamballi, A.K. and Kim, G.S.: *The Strength Characteristics of Aluminium Honeycomb Sandwich Panels, 1999. — 223 p.*
[21] Faulkner D.: *A review of effective plating for use in the analysis of stiffened plating in bending and compression, 1975. — 1-17p*
[22] Kunimoto T, Mori N.: *Study on the buffer characteristics of the corrugated-core used for the 5051 aluminum alloy sandwich construction under dynamic loading, 1989. — 688 p.*
[23] Wierzbicki T.: *Crushing analysis of metal honeycombs, 1983. — 169 p.*
[24] Hexcel.: *Honeycomb sandwich design technology, 1995. — 14 p.*
[25] *Boeing 777-200ER* [Digital source] - Access mode: URL:

https://www.anacargo.jp/en/int/specification/b7_200.html.

Appendices

					NAU 21 20L 00 00 00 50 EN	
Performed by	Liu Kai			Appendices	List	Sheet 69 / Sheets
Supervisor	Yutskevych S.S.					
Adviser						
Stand.contr.	Khizhnyak S.V.				AF 402 134	
Head of dep.	Ignatovych S.R.					

П Р О Е К Т
С А М О Л Е Т А С Т Р Д Д
Н А У, А К И, кафедра К Л А

ПРОЕКТ diploma Расчет выполнен 30.09.20
Исполнитель Liu Kai Руководитель

ИСХОДНЫЕ ДАННЫЕ И ВЫБРАННЫЕ ПАРАМЕТРЫ

Количество пассажиров	500.
Количество членов экипажа	2.
Количество бортпроводников или сопровождающих	13.
Масса снаряжения и служебного груза	5889.71 кг.
Масса коммерческой нагрузки	52250.00 кг.
Крейсерская скорость полета	850. км/ч
Число "М" полета при крейсерской скорости	0.7966
Расчетная высота начала реализации полетов с крейсерской экономической скоростью	11.00 км
Дальность полета с максимальной коммерческой нагрузкой	8000. км.
Длина летной полосы аэродрома базирования	2.20 км.
Количество двигателей	4.
Оценка по статистике тяговооруженности в н/кг	2.6000
Степень повышения давления	30.00
Принятая степень двухконтурности двигателя	4.50
Оптимальная степень двухконтурности двигателя	4.50
Относительная масса топлива по статистике	0.3800
Удлинение крыла aspect ratio	7.39
Сужение крыла taper ratio	3.60
Средняя относительная толщина крыла	0.120
Стреловидность крыла по 0.25 хорд Sweep back angle	30.0 град.
Степень механизированности крыла	1.100
Относительная площадь прикорневых наплывов	0.100

Профиль крыла - Суперкритический
Шайбы УИТКОМБА - установлены
Спойлеры - установлены

Диаметр фюзеляжа	7.00 м.
Удлинение фюзеляжа	10.00
Стреловидность горизонтального оперения	35.0 град.
Стреловидность вертикального оперения	45.0 град.

Р Е З У Л Ь Т А Т Ы Р А С Ч Е Т А
Н А У, А К И, КАФЕДРА "К Л А"

Значение оптимального коэффициента подъемной силы в расчетной точке крейсерского режима полета Су 0.45794

Значение коэффициента Сх.инд. 0.00911

ОПРЕДЕЛЕНИЕ КОЭФФИЦИЕНТА Dм = Мкрит - Мкрейс

Число Маха крейсерское	Мкрейс	0.79660
Число Маха волнового кризиса	Мкрит	0.80863
Вычисленное значение	Dм	0.01203

Значения удельных нагрузок на крыло в кПа (kPa) (по полной площади):

при взлете	5.808
в середине крейсерского участка	4.629
в начале крейсерского участка	5.593

Relative load (wing)

Значение коэффициента сопротивления фюзеляжа и гондол	0.00948
Значение коэфф. профиль. сопротивления крыла и оперения	0.00916

Значение коэффициента сопротивления самолета:

в начале крейсерского режима	0.03060
в середине крейсерского режима	0.02871
Среднее значение Су при условном полете по потолкам	0.45794

Среднее крейсерское качество самолета 15.95329

Значение коэффициента Су.пос.	1.579
Значение коэффициента (при скорости сваливания) Су.пос.макс.	2.368
Значение коэффициента (при скорости сваливания) Су.взл.макс.	1.942
Значение коэффициента Су.отр.	1.418
Тяговооруженность в начале крейсерского режима	0.553
Стартовая тяговооруженность по условиям крейс. режима Ro.кр.	2.301
Стартовая тяговооруж. по условиям безопасного взлета Ro.взл.	2.850

Расчетная тяговооруженность самолета Ro 2.964

Отношение Dr = Ro.кр / Ro.взл Dr 0.807

УДЕЛЬНЫЕ РАСХОДЫ ТОПЛИВА (в кг/кН*ч):

взлетный	38.0281
крейсерский (характеристика двигателя)	59.6602
средний крейсерский при заданной дальности полета	64.7231

ОТНОСИТЕЛЬНЫЕ МАССЫ ТОПЛИВА:

аэронавигационный запас	0.03651
расходуемая масса топлива	0.34558

ЗНАЧЕНИЯ ОТНОСИТЕЛЬНЫХ МАСС ОСНОВНЫХ ГРУПП:

крыла	0.09477
горизонтального оперения	0.00982
вертикального оперения	0.01014
шасси	0.03802
силовой установки	0.09840
фюзеляжа	0.07462
оборудования и управления	0.10408
дополнительного оснащения	0.00748
служебной нагрузки	0.01829
топлива при Lрасч.	0.38210
коммерческой нагрузки	0.16223

Взлетная масса самолета "М.о" = 322080. кГ.

Потребная взлетная тяга одного двигателя 238.67 кН

Относительная масса высотного оборудования и противообледенительной системы самолета	0.0197
Относительная масса пассажирского оборудования (или оборудования кабин грузового самолета)	0.0125
Относительная масса декоративной обшивки и ТЗИ	0.0061
Относительная масса бытового (или грузового) оборудования	0.0177
Относительная масса управления	0.0040
Относительная масса гидросистем	0.0127
Относительная масса электрооборудования	0.0209
Относительная масса локационного оборудования	0.0018
Относительная масса навигационного оборудования	0.0027
Относительная масса радиосвязного оборудования	0.0013
Относительная масса приборного оборудования	0.0031
Относительная масса топливной системы (входит в массу "СУ")	0.0129
Дополнительное оснащение:	
Относительная масса контейнерного оборудования	0.0062
Относительная масса нетипичного оборудования	0.0013

[встроенные системы диагностики и контроля параметров,
дополнительное оснащение салонов и др.]

ХАРАКТЕРИСТИКИ ВЗЛЕТНОЙ ДИСТАНЦИИ

Скорость отрыва самолета	291.34 км/ч
Ускорение при разбеге	2.21 м/с*с
Длина разбега самолета	1476. м.
Дистанция набора безопасной высоты	472. м.
Взлетная дистанция	1948. м.

ХАРАКТЕРИСТИКИ ВЗЛЕТНОЙ ДИСТАНЦИИ
ПРОДОЛЖЕННОГО ВЗЛЕТА

Скорость принятия решения	262.21 км/ч
Среднее ускорение при продолженном взлете на мокрой ВПП	0.92 м/с*с
Длина разбега при продолженном взлете на мокрой ВПП	1827.92 м.
Взлетная дистанция продолженного взлета	2300.17 м.
Потребная длина летной полосы по условиям прерванного взлета	2383.25 м.

ХАРАКТЕРИСТИКИ ПОСАДОЧНОЙ ДИСТАНЦИИ

Максимальная посадочная масса самолета	223459. кг.
Время снижения с высоты эшелона до высоты полета по кругу	21.8 мин.
Дистанция снижения	51.38 км.
Скорость захода на посадку	247.30 км/ч.
Средняя вертикальная скорость снижения	2.00 м/с
Дистанция воздушного участка	516. м.
Посадочная скорость	232.30 км/ч.
Длина пробега	729. м.
Посадочная дистанция	1245. м.
Потребная длина летной полосы (ВПП + КПБ) для основного аэродрома	2079. м.
Потребная длина летной полосы для запасного аэродрома	1768. м.

ПОКАЗАТЕЛИ ЭФФЕКТИВНОСТИ САМОЛЕТА

Отношение массы снаряженного самолета к массе коммерческой нагрузки	2.7624
Масса пустого снаряженного с-та приход. на 1 пассажира	288.67 кг/пас.
Относительная производительность по полной нагрузке	462.67 км/ч
Производительность с-та при макс. коммерч. нагрузке	43040.6 кг*км/ч
Средний часовой расход топлива	11460.891 кг/ч
Средний километровый расход топлива	13.91 кг/км
Средний расход топлива на тоннокилометр	266.281 г/(т*км)
Средний расход топлива на пассажирокилометр	24.5527 г/(пас.*км)
Ориентировочная оценка приведен. затрат на тоннокилометр	0.4938 $/(т*км)